



## 저작자표시-비영리-변경금지 2.0 대한민국

이용자는 아래의 조건을 따르는 경우에 한하여 자유롭게

- 이 저작물을 복제, 배포, 전송, 전시, 공연 및 방송할 수 있습니다.

다음과 같은 조건을 따라야 합니다:



저작자표시. 귀하는 원저작자를 표시하여야 합니다.



비영리. 귀하는 이 저작물을 영리 목적으로 이용할 수 없습니다.



변경금지. 귀하는 이 저작물을 개작, 변형 또는 가공할 수 없습니다.

- 귀하는, 이 저작물의 재이용이나 배포의 경우, 이 저작물에 적용된 이용허락조건을 명확하게 나타내어야 합니다.
- 저작권자로부터 별도의 허가를 받으면 이러한 조건들은 적용되지 않습니다.

저작권법에 따른 이용자의 권리는 위의 내용에 의하여 영향을 받지 않습니다.

이것은 [이용허락규약\(Legal Code\)](#)을 이해하기 쉽게 요약한 것입니다.

[Disclaimer](#)

**Master's Thesis of Science in Agriculture**

**Prokineticin Receptor 1 Activation Ameliorates  
Insulin Resistance in Mouse Skeletal Muscle Cells**

프로키네티신 수용체 1 활성화가 마우스 골격근세포에서 인슐린  
저항성에 미치는 영향에 대한 연구

**February 2020**

**Jongsoo Mok**

**Department of International Agricultural Technology  
Graduate School of International Agricultural Technology  
Seoul National University**

# **Prokineticin Receptor 1 Activation Ameliorates Insulin Resistance in Mouse Skeletal Muscle Cells**

A thesis  
submitted in partial fulfillment of the requirements to the faculty  
of Graduate School of International Agricultural Technology  
for the Degree of Master of Science in Agriculture

By  
Jongsoo Mok

Supervised by  
Prof. Joonghoon Park

Major of International Agricultural Technology  
Department of International Agricultural Technology  
Graduate School of International Agricultural Technology  
Seoul National University

December 2019

Approved as a qualified thesis  
for the Degree of Master of Science in Agriculture  
by the committee members

**Chairman**      **Tae Sub Park, Ph.D.**

**Member**      **Su Cheong Yeom, Ph.D.**

**Member**      **Joonghoon Park, Ph.D.**

---

---

---

## Abstract

Type 2 Diabetes Mellitus (T2DM) is manifested by progressive metabolic impairments especially in skeletal muscle which becomes resistant to insulin. To date, little is known about the mechanisms that control glucose level and insulin resistance in skeletal muscle.

Activation of Prokineticin receptor 1 (Prokr1) appears to improve the obese and the diabetic phenotypes by reducing fat mass, enhancing insulin delivery to target tissues and increasing survival rate against myocardial infarction. However, the peripheral effect of Prokr1 on skeletal muscle has not been studied yet. In this study, we investigated the possible role of Prokr1 in insulin resistance in skeletal muscle using murine myoblast cell line (C2C12) and primary mouse muscular satellite cells.

We examined the expression levels of Prokr1 in C2C12 and satellite cells during myogenic differentiation, and found that Prokr1 was upregulated during myogenic differentiation especially at protein levels. Prokineticin 2 (Pk2), a natural ligand of Prokr1, induced intracellular calcium mobilization in dose-dependent manner, indicating that Prokr1 would be coupled with G<sub>q</sub> protein. Analysis of microarray datasets has been performed to identify differentially expressed genes (DEGs) by Pk2 treatment in human Prokr1-transgenic HEK293T cell line. We have identified 578 DEGs, including 309 downregulated and 296 upregulated ones by Prokr1 activation. Functional enrichment of DEGs identified that the Prokr1 would activate PI3K/Akt

signaling pathway and MAPK/Erk signaling pathway. In vitro experiments confirmed that Prokr1 significantly activated PI3K/Akt signaling pathway in myotubes derived from C2C12 and satellite cells, regardless of the absence or presence of insulin. Furthermore, Prokr1 activation induced to translocate Solute Carrier Family 2 Member 4 (Slc2a4/Glut4) into plasma membrane in myotubes derived from C2C12 and satellite cells. In palmitate-induced insulin-resistant myotubes, Prokr1 activation enhanced insulin-stimulated Akt phosphorylation as well as Glut4 translocation to the plasma membrane, resulted in 2-(N-(7-nitrobenz-2-oxa-1,3-diazol-4-yl) amino)-2-deoxyglucose (2-NBDG) uptake as well. Prokr1-mediated insulin sensitivity was also improved in palmitate-induced insulin resistant myotube. In vivo analysis demonstrated that compared to lean mice, Prokr1 protein level was decreased in skeletal muscle and white adipose tissue of Diet-Induced Obese (DIO) mice, which implied that the level of Prokr1 expression would be relevant to metabolic disorders.

Taken together, these results demonstrate that Prokr1 would be a crucial player in insulin resistance in skeletal muscle, and Prokr1 would be a potential target for treatment of insulin resistance in T2DM.

**Key words:** Prokr1, Mouse, Skeletal muscle, C2C12, Satellite cell, G<sub>q</sub>, p-Akt, Glut4, 2-NBDG, Insulin resistance

**Student number: 2018-21476**

# Contents

Abstract .....	i
Contents .....	iii
List of Tables .....	v
List of Figures .....	vi
List of Abbreviations .....	vii
 Introduction .....	 1
1. Type 2 Diabetes Mellitus (T2DM) and unmet medical needs .....	1
2. Role of skeletal muscle in glucose homeostasis .....	3
3. Pathogenesis of insulin resistance in skeletal muscle .....	4
4. Satellite cells as stem cell in skeletal muscle .....	5
5. Prokineticin receptor 1 (Prokr1) in obesity and cardiovascular disease .....	7
Materials and Methods .....	10
Results .....	19
1. Increased expression level of Prokr1 during myogenic differentiation .....	19
2. Generation of Prokr1 knockout and transgenic cell lines .....	24
3. Transcriptome analyses of Prokr1-activated HEK293T cells .....	30

4. Effect of Prokr1 activation on the PI3K/Akt signaling pathway in myotubes derived from C2C12 cells and satellite cells .....	33
5. Prokr1 activation induces insulin-stimulated Glut4 translocation in insulin-resistant C2C12 and satellite myotubes .....	38
6. Effect of Prokr1 activation on insulin-stimulated glucose uptake in myotubes derived from C2C12 cells and satellite cells .....	43
7. Reduced expression level of Prokr1 in the skeletal muscle of DIO mice .....	47
Discussion .....	50
Conclusion .....	55
Abstract in Korean .....	95
References .....	98

## **List of Table**

Table 1. List of primers used in this study .....	56
Table 2. List of Differentially Expressed Genes (DEGs) in Prokr1-activated transgenic HEK293T cells .....	58
Table 3. List of Kyoto Encyclopedia of Genes and Genomes (KEGG) pathway-enriched genes .....	91
Table 4. Body weight and fasting blood glucose in lean and Diet-Induced Obese (DIO) mice .....	98



## List of Figures

Figure 1. Increased expression level of Prokr1 during myogenic differentiation .....	21
Figure 2. Generation of human Prokr1 knockout and transgenic cell line...	26
Figure 3. Transcriptome analyses of activated Prokr1 .....	31
Figure 4. Effect of Prokr1 activation on the PI3K/Akt signaling pathway in myotubes derived from C2C12 cells and satellite cells.....	35
Figure 5. Prokr1 activation induces insulin-stimulated Glut4 translocation in insulin-resistant C2C12 and satellite myotubes .....	40
Figure 6. Effect of Prokr1 activation on insulin-stimulated glucose uptake in myotubes derived from C2C12 cells and satellite cells.....	43
Figure 7. Reduced expression level of Prokr1 in skeletal muscle of DIO mice .....	48
Figure 8. Schematic summary of Prokr1 signaling pathway for glucose homeostasis in skeletal muscle. ....	54

## **List of Abbreviations**

2-NBDG	2-(N-(7-nitrobenz-2-oxa-1,3-diazol-4-yl) amino)-2-deoxyglucose
AS160	Akt Substrate of 160 kDa
bFGF	basic Fibroblast Growth Factor
CAGR	Compound Annual Growth Rate
cAMP	Cyclic AMP
CEE	Chick Embryo Extract
CI	Confidential Interval
DEGs	Differentially Expressed Genes
DIO	Diet-Induced Obese
DMEM	Dulbecco's Modified Eagle's Medium
DPBS	Dulbecco's Phosphate-Buffered Saline
ECs	Endothelial Cells
EDL	Extensor Digitorum Longus
eGFP	enhanced Green Fluorescent Protein
FACS	Fluorescent-Activated Cell Sorting
FBS	Fetal Bovine Serum
FFA	Free Fatty Acid
FLIPR	Fluorescent Imaging Plate Reader
Glut4	Glucose transporter type 4
GPCR	G Protein-Coupled Receptor

IRS	Insulin-Receptor Substrate
KEGG	Kyoto Encyclopedia of Genes and Genomes
Max-Min	Maximum-Minimum
Mrap2	Melanocortin receptor accessory protein 2
PI3K	PhosphoInositide 3-Kinase
Pk2	Prokineticin 2
Prokr1	Prokineticin receptor 1
RFU	Relative Fluorescence Units
SGLT2	Sodium-dependent Glucose co Transporter 2
Slc2a4	Solute Carrier Family 2 Member 4
T2DM	Type 2 Diabetes Mellitus

## **Introduction**

### **1. Type 2 Diabetes Mellitus (T2DM) and unmet medical needs**

T2DM is a metabolic disease that is becoming more and more prevalent, leading to major public health problems around the world. The International Diabetes Federation estimates that about 387 million people worldwide were diagnosed with T2DM [1]. T2DM is a long-term metabolic disorder of multiple etiologies that is characterized by hyperglycemia, impaired insulin secretion, insulin resistance, inflammation. The effects of T2DM involve long-term damage, dysfunction and failure of renal, cardiovascular and various organs [2]. Currently, the treatment of T2DM remains at the level of symptomatic relief and does not contribute to the prevention of complications including cardiovascular disease. Globally, more than 70% of patients with T2DM died from cardiovascular causes. The prevention and treatment of micro- and macrovascular complications are major goal of care for T2DM [3]. Current diabetes treatments do not meet the medical needs of improving insulin resistance and preventing complications, which are the underlying cause and result of T2DM. For instance, insulin activates insulin receptor activation and signaling pathways in several tissues. Limitation of insulin is lipoatrophy and lipohypertrophy at sites of injection occur. Metformin decreases hepatic glucose production, decreases intestinal absorption of glucose, and improves insulin sensitivity by increasing peripheral glucose

uptake and utilization. Limitation of metformin is vitamin B12 deficiency, which may cause anemia and neuropathy (risk in elderly). Dipeptidyl Peptidase 4 (DPP-4) increases incretin levels (GLP-1 and GIP), inhibiting glucagon release, increasing insulin secretion, reducing gastric emptying, and reducing blood sugar levels. Limitations of DPP-4 inhibitors include gastrointestinal problems, including nausea, diarrhea and abdominal pain. GLP-1 agonists increase GLP1 receptor activity and insulin secretion, decrease glucagon, and delay gastric. GLP-1 agonist has adverse effects such as nausea, vomiting, pancreatitis, and C cell tumor of thyroid [4]. Most of these T2DM therapeutics available at market now are insulin secretagogue in essential and does not meet the underlying cause of T2DM yet.

In contrast, the recently introduced Sodium-dependent Glucose co Transporter 2 (SGLT2) inhibitor for T2DM treatment by preventing glucose reabsorption in kidney is expected to witness a tremendous growth during the forecast period (2019 – 2024) with a Compound Annual Growth Rate (CAGR) of 15.84% in North American market [5]. Even though the glycemic control level of SGLT2 is lower than that of conventional drugs, the SGLT2 inhibitors reduced the risk for a major cardiac event by 11% (hazard ratio, 0.89; 95% Confidential Interval (CI), 0.83–0.96) [6]. This result demonstrates that SGLT2 inhibitor would reduce mortality rate through attenuation of cardiovascular complications. It would give substantial benefit to the T2DM patients not only by regulating blood glucose levels, but also by increasing survival rate and. Therefore, SGLT2 inhibitor appears to fulfill the unmet

medical needs of T2DM drugs. For the next generation T2DM drug development, it is required to improve the insulin resistance and ameliorate the T2DM-related complication. Hence, identification and understanding of therapeutic targets for regulating insulin resistance and complication of T2DM should be a major research focus in T2DM drug research and development.

## **2. Role of skeletal muscle in glucose homeostasis**

Skeletal muscle is a major organ for glucose metabolism in the body and more than 70% of insulin-mediated glucose intake occurs in it. The promotion of glucose uptake in skeletal muscle is an efficient strategy for glycemic control [7]. Glucose uptake in skeletal muscle is mediated by insulin. The insulin signaling pathway in skeletal muscle involves an Insulin-Receptor Substrate (IRS)/phosphoinositide 3-kinase (PI3K)/protein kinase B (AKT) signal. Glucose uptake through insulin stimulation occurs after the hormone binds to insulin receptor [8]. Activated insulin receptor induces autophosphorylation on tyrosine residues. Then, insulin receptor phosphorylates IRS-1 and IRS-2, which activate and dissociate PI3K/Akt [9]. Akt is responsible for triggering Akt Substrate of 160 kDa (AS160) and the activated AS160 serves to translocate Glucose transporter type 4 (Glut4) by increasing the activity of Ras superfamily of small G protein (Rab) to induce the traffic of Glut4-containing vesicles to the plasma membrane [10]. Hence,

these mechanisms of activation and release of Glut4-containing vesicles are important for glucose homeostasis.

### **3. Pathogenesis of insulin resistance in skeletal muscle**

The term insulin resistance refers to insensitive response to insulin stimulation, resulting in insufficient insulin signaling activity and glucose uptake especially in skeletal muscle, white adipose and liver. As mentioned above, insulin promotes glucose uptake into the skeletal muscle in a dose-dependent manner in non-T2DM people. In insulin resistant states, insulin-stimulated glucose uptake in skeletal muscle is significantly reduced [11], [12]. Patients of T2DM are characterized by an increase in plasma free fatty acids (FFA) [13], and high concentration of FFA can directly impair insulin signaling in skeletal muscle. The mechanism underlying palmitate-induced insulin resistance remains unclear; however, it has been proposed that palmitate interferes the ability of IRS-1 to activate PI3K/Akt pathway. Furthermore, several studies showed that palmitate inhibited insulin-stimulated glucose uptake and insulin resistance both in murine skeletal muscle cells and mice, and lowering FFA levels in the plasma significantly improved insulin sensitivity [14], [15]. Taken together, it has been speculated that high concentration of FFA would play a critical role in the pathogenesis of T2DM, especially causing insulin sensitivity in skeletal muscle.

#### 4. Satellite cells as stem cell in skeletal muscle

Half a century ago, Alexander Mauro identified a group of mononucleated cells on the periphery of adult skeletal muscle myofibers by electron microscopy [16]. These cells were named satellite cells due to the location of them between the basal membrane and the sarcolemma of the adult muscle myofibers [17].

Satellite cells serve as myogenic precursors for muscle regeneration.

Regeneration process of skeletal muscle greatly relies on the dynamic interplay between satellite cells and their surrounding microenvironment (stem cell niche) [16]. They can be activated in response to muscle injury, which causes satellite cells proliferation, fusion and differentiation into multinucleated myotubes and then muscle fibers. Satellite cells found in adult tissues can both replicate themselves (self-renewal) and give rise to functional progeny (multipotency). These observations show that satellite cells are the *bona fide* stem cells of muscle [18].

Among the various genes expressed in all quiescent and proliferating satellite cells, Pax7 is considered as a standard biomarker of satellite cells [19]. In intact muscle, satellite cells are sublaminal and mitotically quiescent (G0 phase). Quiescent satellite cells are characterized by their expression of Pax7 but not MyoD or Myogenin [20].



To separate satellite cells from the skeletal muscle, several methodologies have been established. The choice of methods depends largely on the size of the separation and the experiment that results. Small amounts of satellite cells can be produced by physical trituration from single myofiber explants [21] or enzymatic digestion of the pieces of skeletal muscle tissue [22]. Satellite cells can be separated by Fluorescent-Activated Cell Sorting (FACS) from skeletal muscles on a large scale. Single cells can be isolated by enzymatic digestion from skeletal muscle tissue fragments, followed by immunofluorescence labeling of satellite cell-specific surface markers, Pax7 (positive selection) and conclusive cell surface markers for non-satellite cell populations (negative selection) [23].

C2C12 cell line is a subclone [24] of the murine myoblast cell line from C57BL/J mice [25]. C2C12 cell line consists of a pure population of myogenic cells that are rapidly proliferating and differentiating in culture, forming contractile myotubes and synthesizing muscle proteins [26]. As they are easy to handle and widely used, C2C12 cell line is preferentially chosen for conventional experimental purposes. Nonetheless, as they have lost the true characteristics of the original tissue from which they were isolated [27], it is doubtful to use C2C12 cell line as a biologically relevant *in vitro* model. In contrast, primary murine muscular satellite cells have natural morphology of the cells and retain many of the primary markers and functions. Because of the higher relevance to the *in vivo* condition, muscular satellite cells are considered to be a superior *in vitro* model than C2C12 cell line [28].

However, primary murine muscular satellite cells usually have a limited lifespan and they are a mixture of different cells at different stage in nature. To continue a more uniform culture, it is necessary to purify certain types of cells. Although there are several limitations of the primary murine muscular satellites cells, they are superior to stable cell line in various biological aspects, and could reproduce the muscle physiology.

## **5. Prokineticin receptor 1 (Prokr1) in metabolic disorders**

Prokr1 is the first non-melanocortin G Protein-Coupled Receptor (GPCR) to be regulated by Melanocortin receptor accessory protein 2 (Mrap2), which inhibits specifically Prokr1 signaling pathway [29]. Prokineticin 2 (Pk2) is a natural ligand of Prokr1, which is a potent angiogenic [30] and anorexigenic hormone [31]. Pk2 has binding affinity to two similar GPCRs – Prokr1 and Prokineticin receptor 2 (Prokr2), but the binding affinity to Prokr1 is much higher than Prokr2 [32]. Pk2 is expressed in various organs and/or cells including monocytes, macrophages, reproductive track [33], adipose tissue, heart and kidney [34], [35], [36].

Obesity can be manifested by increased body fat mass and inflammation in white adipose tissue [37]. Prokr1 activation suppresses proliferation and adipogenesis of preadipocytes [34]. In whole body or adipose tissue specific Prokr1-deficient (Prokr1<sup>ad-/-</sup>) mice, excessive accumulation of abdominal fat mass was found due to the expansion of white adipose tissue in both

genetically engineered mice by new adipocyte formation [34]. Furthermore, decreased expression of Prokr1 in adipocytes contributed to the development of T2DM-like phenotypes including increased fasting glucose level, decreased circulating insulin level and impaired glucose tolerance.

Angiogenesis plays a major role in modulating the insulin sensitivity in white adipose [38]. Endothelial-specific Prokr1 knockout mice (Prokr1<sup>ec-/-</sup>) show insulin resistance in adipocytes [30], and defect in insulin delivery process via Endothelial Cells (ECs) contributes to insulin resistance [39]. Therefore, the vascular endothelium is considered a potential therapeutic target for prevention of insulin resistance and related complications [40]. Prokr1<sup>ec-/-</sup> mice had impaired capillary formation and poor transcapillary absorption of insulin, which is rescued by adenoviral transfection of the Prokr1 gene [30]. In contrast, Prokr1 transgenic mice enhance insulin transendothelial delivery and angiogenesis [41].

Peripheral administration of Pk2 reduces the circulating level of plasma insulin and improves insulin sensitivity in Diet-Induced Obese (DIO) mice [31]. These data emphasize the role of Prokr1 as a successful insulin delivery regulator and increases insulin sensitivity.

Prokr1 plays an important role particularly in cardiac progenitor cell commitment and cell-to-cell communication as well [42]. Prokr1 signaling protects cardiomyocytes against hypoxia-mediated apoptosis by activating the Akt signaling pathway [35]. In addition, activation of the cardiac Prokr1

upregulates its own Pk2 to induce the differentiation of the epicardial progenitor cell (EPDC) into endothelial cells to facilitate neovasculogenesis [42]. Interestingly, Prokr1 null mice have defects in cardiomyocyte contractile and prone to apoptosis due to lack of Prokr1 signaling in part [36]. These finding indicate that Prokr1 in cardiomyocyte is important for cardiomyocyte survival and cell-autonomous contractility. Prokr1 in cardiomyocyte drives EPDCs proliferation and differentiation. Prokr1 activates Akt and MAPK in cardiac ECs to enhance proliferation, angiogenesis and migration. The loss of Prokr1 in ECs leads to defective angiogenesis [30]. Therefore, Prokr1 appears to have regulatory effects on adipogenesis, insulin sensitivity by modulating insulin delivery, and protection of cardiomyocyte defects.

The metabolic effects of Prokr1 in the skeletal muscle are largely unknown. In this study, we investigated the potential role of Prokr1 in insulin resistance in skeletal muscle using murine myoblast cell line (C2C12) and primary mouse muscular satellite cells.

## **Materials and Method**

### **Animal tissues**

Liver, brown adipose, white adipose, and skeletal muscle tissues of male C57BL6/J mice were generously provided by Hyundai Pharma Co. (Yongin, Kyunggi-do, Korea)

The mice at 4 weeks old were fed either by normal (10 kcal% fat) or high-fat (60 kcal% fat) diet for 52 weeks. Tissues were collected after humane sacrifice and delivered to in-house storage at -80°C until use.

### **Generation of genetically engineered cells**

To establish human Prokr1-overexpressing HEK293T cells, human Prokr1 expressing piggyBac transposon (Systems Biosciences, Palo Alto, CA, USA) using Lipofectamine 3000 (Invitrogen, Carlsbad, CA, USA) according to the manufacturer's protocol. Once the seeded cells reached 80% confluency on 6-well culture plates, they were washed with Dulbecco's Phosphate-Buffered Saline (DPBS) (Gibco, Grand Island, NY, USA) and refreshed with 2 mL of Dulbecco's Modified Eagle's Medium (DMEM; Gibco) without antibiotic-antimycotic. The piggyBac transposon-lipid complex consisting of 7.5 uL Lipofectamine 3000 reagent, 10 uL P3000 reagent and 2.5 ug piggyBac transon in 250 uL Opti-MEM (Invitrogen) was added to each well. One day

after lipofection, 10 ug/ mL puromycin (Gibco) was added to select the cells stably transfected with the transgene. Transgene analysis was performed using three methods: DNA sequencing, qRT-PCR and western blot.

To knockout the human Prokr1 gene in HEK293T cells, a guide RNA (gRNA) expressing vector and a Cas9 expressing vector carrying the enhanced Green Fluorescent Protein (eGFP) gene (Sigma, St. Louis, MO, USA) were co-transfected at a ratio of 1:1 (2.5 µg each) using Lipofectamine 3000 (Invitrogen) according to the manufacturer's instruction. One day after lipofection, HEK293T cells were harvested and resuspended in DPBS (Gibco) containing 1% Bovine Serum Albumin (BSA; Sigma) and passed through a 40 µm cell strainer (Becton, Dickinson and Company, Franklin Lakes, NJ, USA) for fluorescence-activated cell sorting using FACS Aria<sup>TM</sup> III cell sorter (Becton, Dickinson and Company). After enrichment of GFP-positive cells, GFP-positive single cell was picked under a microscope and seeded onto individual wells of a 96-well plate (Thermo Fisher Scientific, Waltham, MA, USA). Transgene analysis was performed using two methods: DNA sequencing and western blot.

### **Isolation of muscular satellite cells**

Satellite cells were isolated from skeletal muscle samples and cultured as previously described [43]. C57BL/6 J female mice at 4 weeks old were humanely sacrificed and Extensor Digitorum Longus (EDL) muscle tissue

was removed and digested in 0.2% (w/v) Collagenase Type 1 (Sigma) for 1 hr at 37°C. The digested tissue was physically dissociated using 15 mL syringe equipped with 18G needle (Korea Vaccine, Ansan, Kyunggi-do, Korea) and then digested again in 0.2% (w/v) collagenase type 1 (Sigma) for 15 min at 37°C. The physically dissociated and enzymatically digested muscle tissue was filtered through 70  $\mu$ m and 40  $\mu$ m cell strainer (Sigma) sequentially. The cell filtrate was subject to centrifuge at 1,000 rpm for 15 min, and the pellet was seeded on 0.1% (v/v) Collagen Type 2-coated 100 mm tissue culture plate (Thermo Fisher Scientific) for three days under 5% CO<sub>2</sub> condition at 37°C. To enrich the satellite cells, the seeded cells were harvested by 0.25% Trypsin in 1 mM EDTA (Gibco) and allowed to settle down for 30 min to remove fibroblast cells twice. Then the supernatant after settlement was transferred to 0.1% (v/v) Collagen Type 2-coated 100 mm tissue culture plate (Thermo Fisher Scientific) and maintained under 5% CO<sub>2</sub> condition at 37°C until use.

### **Preparation of Chick Embryo Extract (CEE)**

CEE were extracted according to the method described by Kristian *et al.* [44]. Briefly, chick embryos at 11 days old were blended with 50 mL syringe without needle (Korea Vaccine) and mixed with cold DMEM (Gibco) at a ratio of 1:1. The mixture was subject to ultracentrifuge to remove larger particles and debris at 180,000 g, 4°C for 6 hr. The supernatant was subject to

filtration through 0.45  $\mu$ m and 0.22  $\mu$ m bottle top filter (Invitrogen) subsequently. Sterile CEE was aliquoted, and then kept at -80°C until use.

### **Cell maintenance, differentiation and treatment**

C2C12 cell line (ATCC, Manassas, VA) were maintained in DMEM (Gibco) with 20% Fetal Bovine Serum (FBS) (Gibco) under 5% CO<sub>2</sub> condition at 37°C and differentiated in DMEM with 2% horse serum (Gibco) after reaching 80% confluence. After 6 days, the myoblasts were differentiated into myotubes. Primary mouse muscular satellite cells were maintained in DMEM (Gibco) with GlutaMax (Gibco), 20% FBS (Gibco), 1 ng/mL basic Fibroblast Growth Factor (bFGF) (Invitrogen, Carlsbad, CA, USA), 1% Chick Embryo Extraction (CEE) at 37°C under 5% CO<sub>2</sub> condition at 37°C. Differentiation was induced at 80% confluence, using differentiation medium with 2% horse serum (Gibco) media for 3 days.

Myotubes were incubated with 0.2 mmol/L palmitate (Sigma) for 8 hr to induce insulin resistance [45]. Cells were then treated with Pk2 (Sigma, 10 nmol/L) dissolved in DPBS (Gibco) or DPBS (Gibco) alone in the presence or absence of indicated inhibitors for 30 min. At the end of treatment, cells were stimulated with 100 nmol/L insulin (Cell applications, Inc. San Diego, CA, USA) or DPBS (Gibco) for 10 min before total protein or membrane protein were extracted.



### **Calcium mobilization assay**

Calcium sensitive Fluorescent Imaging Plate Reader (FLIPR) Calcium 6 assay dye (Molecular Devices, CA, USA) was added to each well of a 96-well plate containing HEK293T and C2C12 cell line. Cells were seeded the night before the experiment at a concentration of 50,000 cells/ well in a volume of 100  $\mu$ L per well of black walled. The cells were incubated for 1 hr prior to the recording of intracellular calcium levels in a FlexStation3 Multi-Mode Microplate Reader (Molecular Devices) as previously described [46]. All compounds were diluted in calcium buffer made with 1x HBSS (Thermo Fisher Scientific), 20 mM HEPES (Thermo Fisher Scientific), and 2.5 mM Probenecid (Sigma). For agonist studies, Pk2 (Sigma) was diluted in DPBS (Gibco) containing calcium buffer at desired concentrations and was added during the recording. The same amount of DPBS (Gibco) was added to all control groups to maintain similar DPBS (Gibco) levels with the experimental groups. Relative Fluorescence Units (RFU) were measured for 120 seconds period by the Flexstation3. Maximum-Minimum (Max-Min) was further evaluated from individual calcium data.

### **Cyclic AMP (cAMP) assay**

cAMP levels were measured by the cAMP Direct Immunoassay Kit (ab65355) (Abcam, Cambridge, MA, USA) following Abcam's protocol, and optical density at 450 nm were measured in the cell lysates of HEK293T cell line.

### **Measurement of 2-[N-(7-nitrobenz-2-oxa-1,3-diazol-4-yl) amino]-2-deoxy-D glucose (2-NBDG) uptake**

Glucose uptake activity was measured using 2-NBDG (Thermo Fisher Scientific), a fluorescent D-glucose analogue, in C2C12 cells as a previously described method with slight modifications. Briefly, differentiated muscle cells on 24-well plates were treated with different kinds of BSA (Sigma) - conjugated palmitate (Sigma) for 8 hr. After 2 hr incubation in no glucose DMEM, myotubes were incubated with or without 100 nM insulin (Cell applications, Inc.) for 1 hr. Next, myotubes were transferred to fresh no glucose DMEM medium supplemented with 80 uM fluorescent deoxyglucose 2-NBDG (Thermo Fisher Scientific) for 30 min. After three times washed by DPBS, The fluorescence intensity of cellular 2-NBDG (Thermo Fisher Scientific) in each well was measured at an excitation wave-length of 485 nm and an emission wavelength of 535 nm using Cytation 5, Multi-Mode Reader (BioTek, Canada).

## qRT-PCR

Total RNA was prepared sample using a RNeasy Mini kit (QIAGEN, Venlo, The Netherlands) according to the manufacturer's instructions. Total RNA (5 ug) was reverse transcribed with Super Script III Reverse Transcription Reagents (Invitrogen). cDNA was subjected to real-time quantitative PCR, in which a specific primer for mouse *Pax7*, *Myf5*, *Myod1*, *Mb*, *Myog*, *Myh2*, *Myh7*, *Prokr1*, human *Prokr1*, *Prokr2*. Primers referred were summarized in Table 1. The real-time PCR was carried out in an SYBR green (Applied Biosystems, Foster City, CA, USA). Relative values of mRNAs were analyzed by the  $\Delta\Delta C(T)$  method, normalized to *Gapdh* mRNA and shown as fold change in expression over control.

## Western blotting

Total protein concentration in the supernatant was determined using a BCA Protein Assay Reagent kit (Thermo Fisher Scientific). Lysate containing 30  $\mu$ g total protein was loaded into each well and separated by dodecyl sulfate-poly acrylamide electrophoresis. Thereafter, proteins were transferred to nitrocellulose membranes that were subsequently incubated in 5 % BSA (Sigma) containing primary antibodies against Prokr1 (1:1000), Akt (1:1000), phospho-Akt (1:1000), Erk (1:1000), phospho- Erk (1:1000), and Glut4

(1:500) (Santa Cruz Inc., Santa Cruz, CA) and at 4°C overnight. After three times washing, the membranes were incubated with anti-rabbit secondary antibody for 1 hr at room temperature and washed three times with TBST for 15 min. Blots were detected by an enhanced chemiluminescence kit (Biorad, Inc. Berkeley, California, USA). Band density was measured by ImageJ (version 1.80v, NIH). Prokr1 content in samples were calculated and normalized using Actb (Santa Cruz) as an internal control. Western blot analysis was performed to quantify the expression level of Glut4 in the cell membrane. Glut4 levels were normalized by Na<sup>+</sup>/K<sup>+</sup>-ATPase alpha (1:200) (Santa Cruz), which is a known plasma cell membrane marker [47].

### **Immunocytochemistry (ICC)**

After washing with DPBS (Gibco), cells were fixed with 10% neutral buffered formalin (Sigma) in DPBS (v/v) (Gibco) for 10 min at 25°C. Rinse briefly with DPBS (Gibco). Permeabilized with 0.5% Triton X-100 (Sigma) for 10 minutes and blocked with 5% BSA in DPBS (v/v) for 1 hr at 25 °C. The expression of Glut4 was detected using anti-Glut4 antibody (1:200) (Santa Cruz) overnight at 4 °C, followed by Alexa Fluor 488-goat anti-mouse IgG antibody (1:1000) (Life Technologies, Eugene, OR, USA) for 1hr at 25 °C. Cells were visualized under a fluorescence microscope using Cytation 5, Multi-Mode Reader (BioTek).

## **Microarray analysis**

Following quantitative and qualitative evaluations performed with BioAnalyzer (Agilent, Santa Clara, CA, USA), RNA samples with an RNA integrity number (RIN)  $\geq 6.7$  and A260/A280 values  $\geq 1.88$  were subjected to cDNA synthesis, performed with the GeneChip WT cDNA synthesis and amplification kit (Applied Biosystems). Next, the cDNA was fragmented and biotin-labeled using GeneChip WT terminal labeling kit (Applied Biosystems), and approximately 5.5  $\mu\text{g}$  of labeled cDNA was hybridized to the Affymetrix GeneChip Human Gene 2.0 ST Array (Affymetrix, Santa Clara, CA, USA) at 45 °C for 16 h. The hybridized arrays were scanned on a GCS3000 Scanner (Affymetrix) and all data analyses were performed with the GeneChip Command Console Software (Affymetrix).

## **Statistical analyses**

All data were analyzed with Student t-tests depending on the homogeneity of variance of the data. All statistical analyses were performed using Prism software (ver. 7.03; GraphPad Software, Inc., San Diego, CA, USA) with p-values  $< 0.05$  considered to indicate statistical significance. All measurements are reported as means  $\pm$  standard deviation (SD) or standard error of the mean (SEM).

## Result

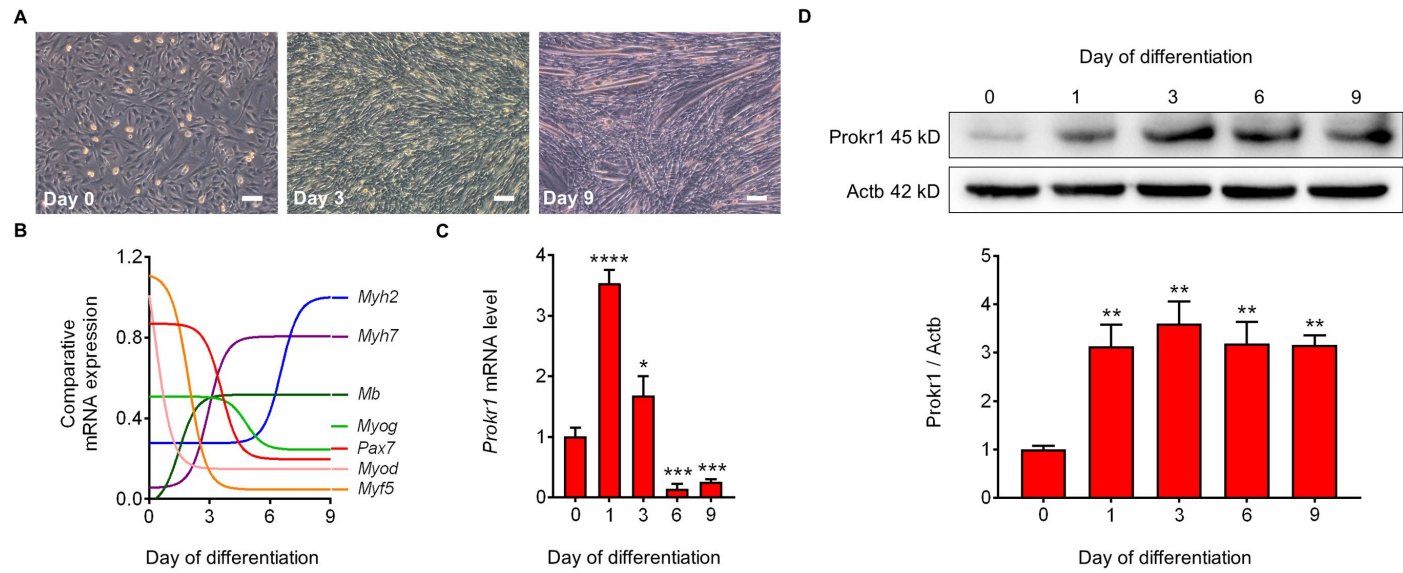
### 1. Increased expression level of Prokr1 during myogenic differentiation

To understand the functional role of Prokineticin receptor 1 (Prokr1) during myogenesis, expression levels of myogenic markers and Prokr1 were investigated throughout myogenic differentiation of murine myoblast C2C12 cells and primary mouse muscular satellite cells.

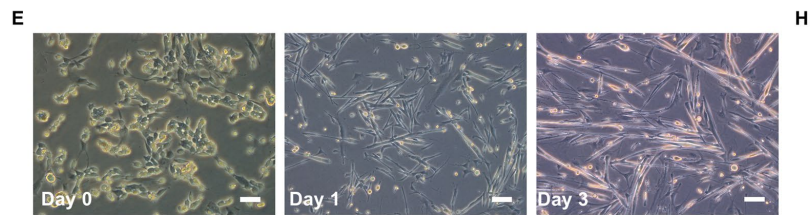
Mononucleated C2C12 cells at 90% confluency were subjected to myogenic differentiation (Day 0). After 3 days of induction, cell morphology started to be changed and became elongated, multinucleated myotubes on Day 9 (Fig. 1A). In parallel with C2C12 cells, mononucleated satellite cells at Day 0 were subjected to myogenic differentiation. One day after induction, satellite cells gradually differentiated into fused myocytes, and visible myotubes were appeared on 3 days of induction (Fig. 1B). Morphological changes of muscular satellite cells were comparable to those of C2C12 cells, but were faster than C2C12 cells. During myogenic differentiation, mRNA levels of myoblast marker genes (*Myf5*, *Myod*, *Pax7*) were gradually decreased and myotube markers (*Myh2*, *Myh7*, *Mb*) were increased as previously reported findings [48] (Fig. 1C-D). *Prokr1* mRNA in C2C12 cells transiently increased at Day 1, and then gradually decreased during myogenesis (Fig. 1E). These expressional dynamics of *Prokr1* mRNA was reproduced in muscular satellite cells as the expression level was reduced during

myogenesis (Fig. 1F). In contrast to the mRNA expression, the protein level of Prokr1 in C2C12 cells was significantly increased at Day 1, and then maintained throughout myogenesis (Fig. 1G). In consistent with these findings, the level of Prokr1 protein in the muscular satellite cells was increased on Day 3 of myogenic differentiation (Fig. 1H).

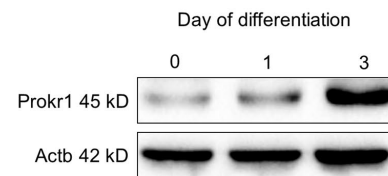
Taken together, these results demonstrate that the expression level of Prokr1 appears to be increased in mature myotubes from both of C2C12 cells and muscular satellite cells, which implies putative physiological role of Prokr1 in mature myotubes.



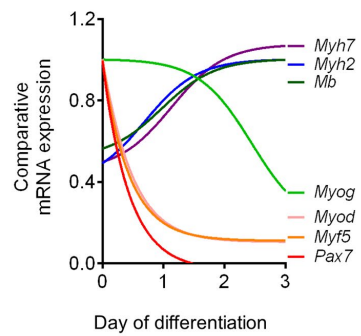




**H**



**F**



**G**

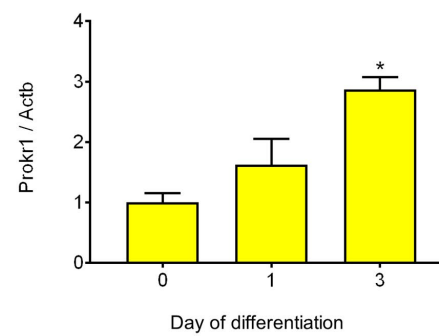
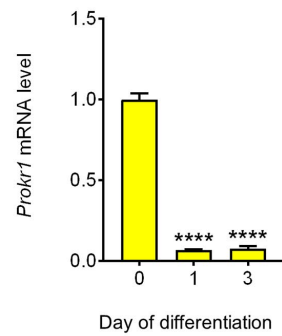


**Figure 1. Increased expression level of Prokr1 during myogenic differentiation**

**A.** Morphological change of C2C12 myoblasts differentiating into myotubes at the post induction Day 0 (proliferating myoblasts), Day 3 (mononucleated myocytes) and Day 9 (long multinucleated myotubes). Scale bar = 100  $\mu$ m.

**B.** Expression dynamics of myogenic marker genes in C2C12 cells. Relative expression levels were calculated based on maximum expression level = 1.

**C.** Expression dynamics of Prokr1 mRNA in C2C12 cells. Mean  $\pm$  SD, n = 3, \* $p$  < 0.05, \*\*\* $p$  < 0.001, \*\*\*\* $p$  < 0.0001 vs. Day 0.

**D.** Expression dynamics of Prokr1 proteins during myogenesis in C2C12 cells. Mean  $\pm$  SEM, n = 3, \*\* $p$  < 0.001 vs. Day 0.

**E.** Morphological change of satellite cell differentiating into myotubes at the post-induction Day 0 (proliferating satellite cells), Day 1 (fused myocytes), Day 3 (long multinucleated myotubes). Scale bar = 100  $\mu$ m.

**F.** Expression dynamics of myogenic marker genes in satellite cells. Relative expression levels were calculated based on maximum expression level = 1.

**G.** Expression dynamics of Prokr1 mRNA during myogenesis in satellite cells. Mean  $\pm$  SD, n = 3, \*\*\*\* $p$  < 0.0001 vs. Day 0.

**H.** Expression dynamics of Prokr1 proteins during myogenesis in satellite cells. Mean  $\pm$  SEM, n = 3, \*\* $p$  < 0.001 vs. Day 0.

## 2. Generation of Prokr1 knockout and transgenic cell lines

G Protein-Coupled Receptors (GPCRs) convert a wide variety of extracellular signals by binding various G proteins including  $G_{q/11}$ ,  $G_s$ ,  $G_{i/o}$ , or  $G_{12/13}$  for transducing a variety of intracellular messages [49]. For example, GPCRs coupled to  $G_{q/11}$  results in calcium release from endoplasmic reticulum [50], whereas, GPCRs coupled to  $G_s$  results in cyclic AMP (cAMP) accumulation.

To identify Prokr1 coupled protein, we performed calcium mobilization assay and cAMP assay. First, calcium mobilization assay was performed, in C2C12 cell line. it was significantly reacted in Pk2 100 nM (Fig. 2H). However, there was a limit to reacting at too high a concentration. Therefore, we made human Prokr1 overexpressed transgenic cell line in HEK293T (HEK293T<sup>Prokr1</sup>) and knockout cell line in HEK293T cell line were examined by sequencing (Fig. 2A) Western blot and qRT-PCR.

In the naïve, mock, and knockout cell line, mRNA level of human Prokr1 was weak from agarose gel. However, mRNA level of human Prokr1 was remarkably appeared in HEK293T<sup>Prokr1</sup> (Fig. 2D). Quantitatively measured HEK293T<sup>Prokr1</sup> significantly increased 7,500-fold mRNA level of human Prokr1 (Fig. 2F). However, Protein level of human Prokr1 prominently increased in HEK293T<sup>Prokr1</sup> (Fig. 2E). Dose-dependent calcium mobilization was observed by Pk2 in HEK293T<sup>Prokr1</sup>. Calcium mobilization significantly increased 1,50-fold at above 1 nM of Pk2 and saturation of calcium

mobilization began at a concentration of 10 nM (Fig. 2G). However, Stimulation of receptors coupled to G<sub>s</sub>-proteins showed a tendency, but not significant. (Fig. 2I).

Taken together, these results demonstrate that Prokr1 is a G<sub>q</sub>-coupled receptor, but G<sub>s</sub>-coupled receptor needs research.

**A**

```

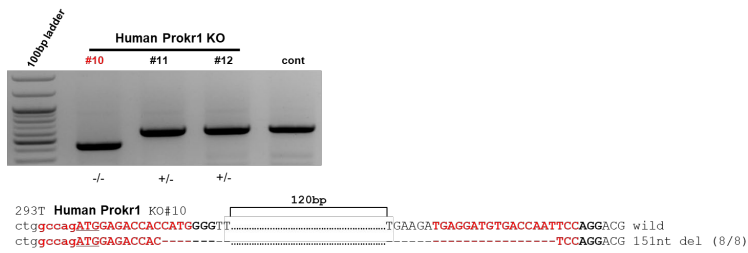
forward primer
gagctcagat accatacccc aaagatgctg gcagagacat tctgactcat 68645721
taagggagag ctggctgata gcagagaggg gtgacatcag ccttgacagac 68645771

PAM
attgccctgg ggaatttga gcagtgttgc tcacagcacc acctggccag 68645821
ATGGAGACCA CCATGGGTT CATGGATGAC AATGCCACCA ACACTTCCAC 68645871
CAGCTTCCTT TCTGTGCTCA ACCCTCATGG AGCCCATGCC ACTTCTTCC 68645921

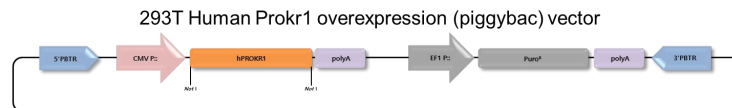
PAM
CATTCAACTT CAGCTAAGC GACTATGATA TGCCTTTGGG TGAAGATGAG 68645971
GATGTGACCA ATTCAGGAC GTTCTTTGCT GCCAAGATTG TCATTGGGAT 68646021
GGCCTGGTG GGCATCATGC TGGTCTGGG CATTGGAAGC TTCATCTTTA 68646071
TGCTGGCCT GGTCCGCTAC AAGAAACTGC GCACCTCAG CACCTGCTC 68646121
ATGCCAAGC TGGCCATCTC TGAATTCTG GTGGCCATG TCTGCTGCC 68646171
CTTGAGATG GACTACTATG TGGTGCCCA GCTCTCCTG GAGCAGGCC 68646221
ACGTCCTGTG CACCTCTGTC AACTACCTGC GCACTGTCTC TCTCTATGTC 68646271
reverse primer
TCCACCAATG CCCTGCTGGC CATGCCATT GACAGgtgag tgcagcagca 68646321

```

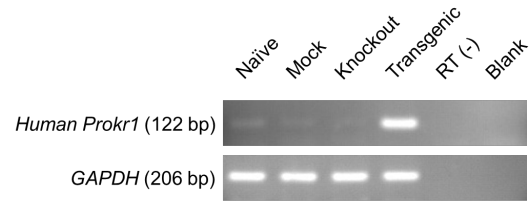
**B**



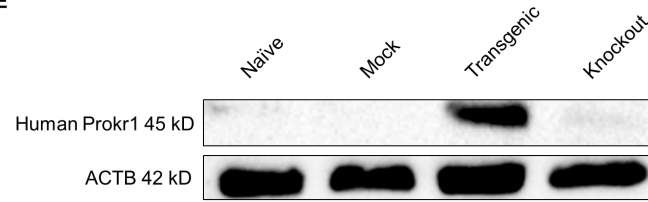
**C**



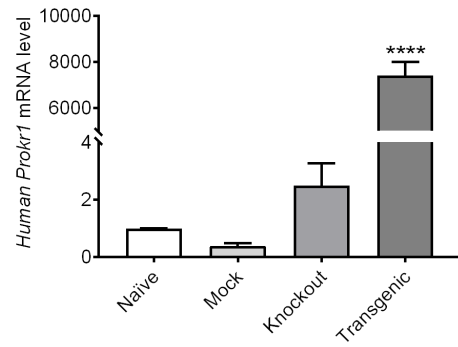
D



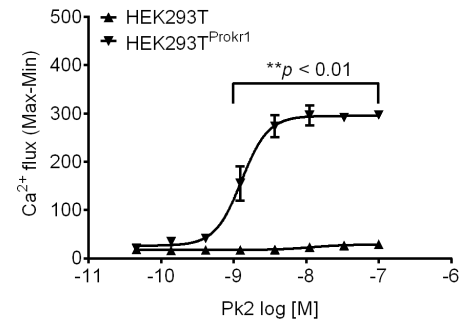
E



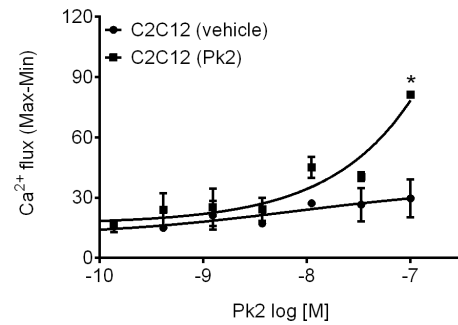
F



G



H



I

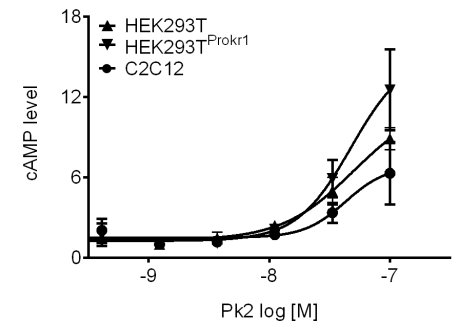


## **Figure 2. Generation of human Prokr1 knockout and transgenic cell lines**

**A.** The blue sequences indicate forward primer and reverse primer for PCR validation. The red sequences are targeted sites of gRNA #1 and gRNA #2, and the bold GGG and AGG sequences are Protospacer Adjacent Motif (PAM).

**B.** Two of HEK293T cell clones (#11 and #12) are identified heterozygous knockout. The other one clone (#10) is homozygous knockout harboring 151 nt deletion in human Prokr1 gene.

**C.** PiggyBac vector construct for human Prokr1 expression is depicted.

**D.** mRNA expression of human Prokr1 is verified by RT-PCR from naïve, mock control treated with empty vector, CRISPR/Cas9-mediated knockout, and piggyBac-mediated transgenic cell lines.

**E.** Protein expression of human Prokr1 is verified by Western blot from naïve, mock control treated with empty vector, piggyBac-mediated transgenic, and CRISPR/Cas9-mediated knockout cell lines.

**F.** mRNA levels of human Prokr1 are quantified by RT-qPCR from naïve, mock control treated with empty vector, CRISPR/Cas9-mediated knockout, and piggyBac-mediated transgenic cell lines. Bars indicate mean  $\pm$  SD,  $n = 3$ . \*\*\*\* $p < 0.0001$  vs. naïve HEK293T cells.

**G.** Cellular function of human Prokr1 in piggyBac-mediated transgenic HEK293T cells is characterized by a calcium mobilization assay at different

concentrations of Pk2. Graphs indicate mean  $\pm$  SD,  $n = 2$ .  $**p < 0.01$  vs. naïve HEK293T cells.

**H.** Cellular function of mouse Prokr1 in C2C12 cells is characterized by a calcium mobilization assay at different concentrations of Pk2. Graphs indicate mean  $\pm$  SD,  $n = 2$ .  $*p < 0.05$  vs. vehicle-treated C2C12 cells.

**I.** Cellular function of human or mouse Prokr1 in naïve HEK293T, piggyBac-mediated transgenic HEK293T, or C2C12 cells is characterized by a cAMP assay at different concentrations of Pk2. Graphs indicate mean  $\pm$  SD,  $n = 3$ .



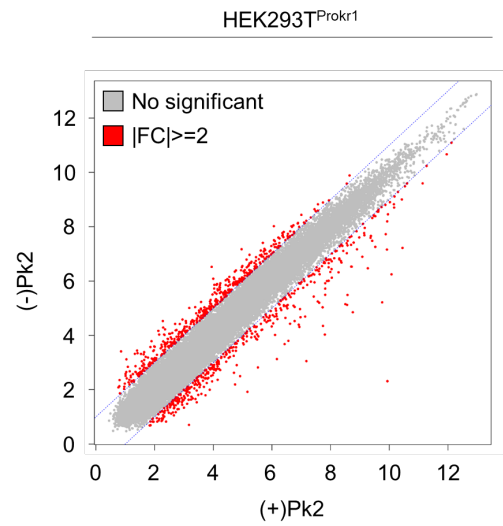
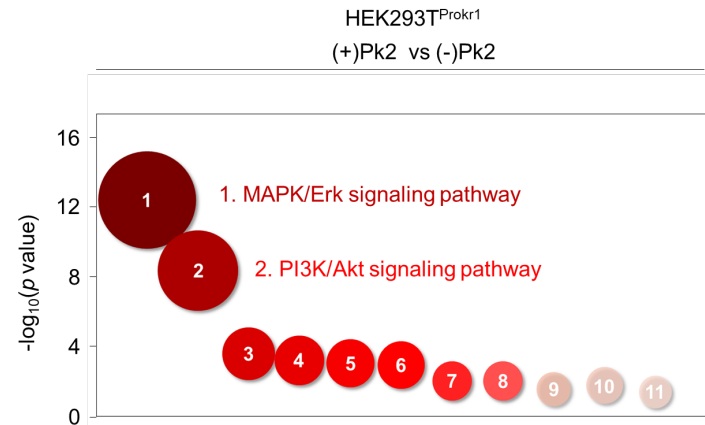
### **3. Transcriptome analyses of Prokr1-activated HEK293T cells**

To get insight of molecular mechanism of Prokr1, we investigated transcriptomic response of activated HEK293T<sup>Prokr1</sup> cells.

We identified 578 DEGs, including 269 upregulated and 309 downregulated genes, in activated HEK293T<sup>Prokr1</sup> cells by Pk2 treatment (Fig. 3A, Table 2).

KEGG pathway analysis was performed to determine the functional enrichment of 578 genes and identified that MAPK-Erk signaling pathway and the PI3K-Akt signaling pathway were significantly altered by Prokr1 activation (Fig. 3B and Table 3).

These findings suggest that MAPK/Erk signaling pathway and PI3K/Akt signaling pathway would be putative signaling pathways dominantly altered by Prokr1 activation.

**A****B**

### **Figure 3. Transcriptome analyses of Prokr1-activated HEK293T cells**

**A.** Expression level of each gene in HEK293T<sup>Prokr1</sup> cells with or without Pk2 treatment is depicted in scatter plot. Gray dots indicate genes without fold difference. Red dots indicate differentially expressed genes (DEGs) with fold change cutoff = 2. (+)Pk2 = HEK293T<sup>Prokr1</sup> with Pk2 treatment, (-)Pk2 = HEK293T<sup>Prokr1</sup> without Pk2 treatment. X- and y-axis is normalized expression level of each condition.

**B.** Functions enriched with DEGs in Pk2-treated HEK293T<sup>Prokr1</sup> cells are depicted as advanced bubble chart with  $-\log_{10}(\text{p-value})$  as diameter. Rank order of KEGG (Kyoto Encyclopedia of Genes and Genomes) Pathways enriched is indicated in x-axis, and  $(-)\log_{10}$  transformed p-value is represented by the y-axis.

#### **4. Effect of Prokr1 activation on the PI3K/Akt signaling pathway in myotubes derived from C2C12 cells and satellite cells**

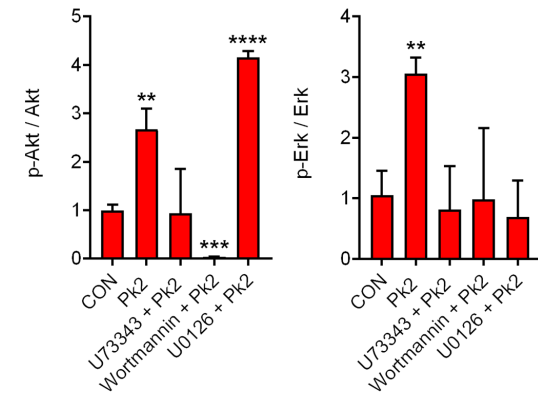
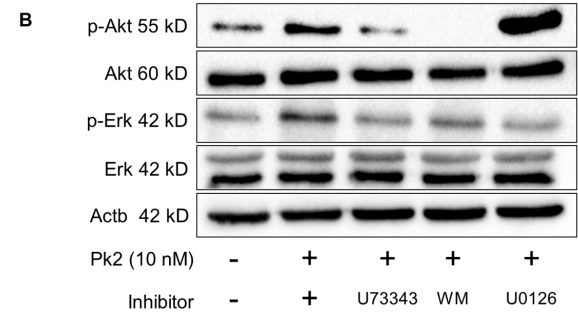
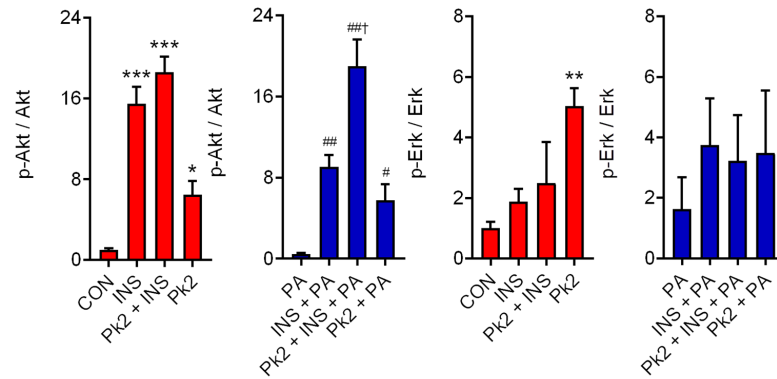
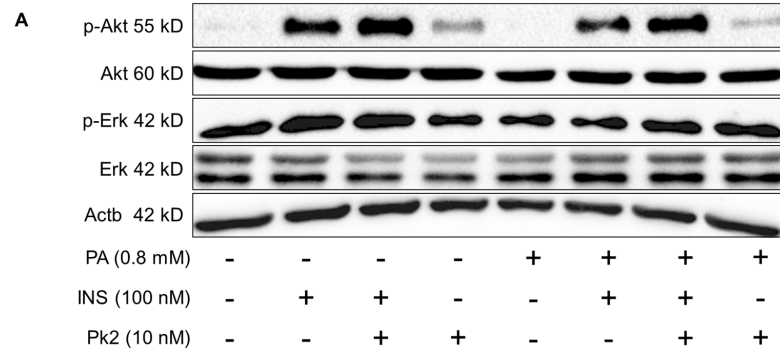
To investigate the effect of Prokr1 activation on insulin resistance and its underlying mechanism, we examined the Prokr1 signaling pathway by measuring Akt and Erk phosphorylation in insulin sensitive (without palmitate) and palmitate-induced insulin-resistant C2C12 myotubes and satellite myotubes.

In C2C12 and satellite myotubes in insulin sensitive, the phosphorylation of Akt was increased by ~15-fold 5-fold after acute insulin stimulation.

Compared to insulin sensitive myotubes, insulin resistant myotubes reduced insulin-induced phosphorylation of Akt by about 40% in C2C12 and satellite myotubes, which could be enhanced by Pk2 treatment. Cotreatment Pk2 with insulin did restore the insulin-induced phosphorylated Akt in both myotubes to insulin sensitive myotubes levels compared with those exposed to palmitate. Furthermore, the phosphorylation of Akt was increased by ~5-fold with treated Pk2 in both insulin sensitive myotubes and insulin resistant myotube. The phosphorylation of Erk was increased by ~4-fold after with treated Pk2. However, there was not clear between Pk2 and insulin and insulin resistance (Fig. 4A, B). These effects of Pk2 on expression of phosphorylated Akt was abolished in the presence of either PLC $\beta$  inhibitor U73343 or PI3K inhibitor wortmannin but Erk inhibitor U0126 did not block the effects of Pk2. The effects of Pk2 on of phosphorylated Erk was abolished

by PLC $\beta$  inhibitor U73343 or PI3K inhibitor wortmannin or Erk inhibitor U0126. (Fig. 4C, D).

These findings suggest that Pk2 would improve insulin resistance in myotube through PLC $\beta$ /PI3K/Akt pathway. However, the effect of MAPK/Erk pathway in insulin resistant appears to be negligible in C2C12 and satellite myotubes.



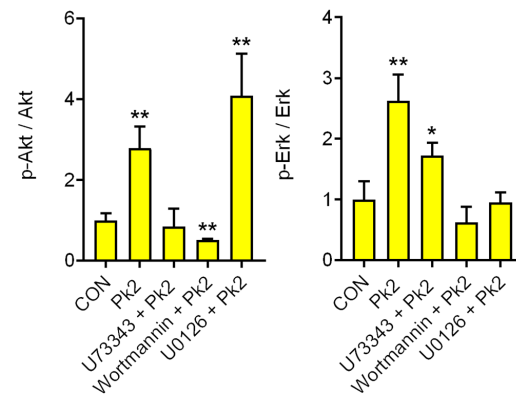
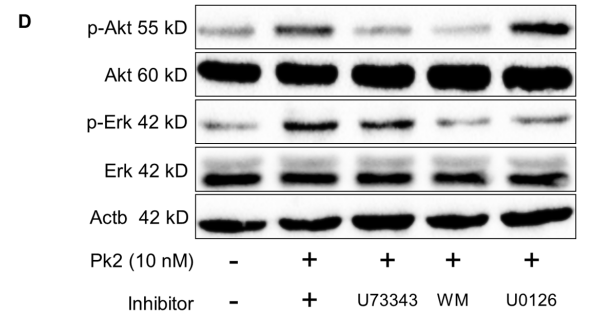
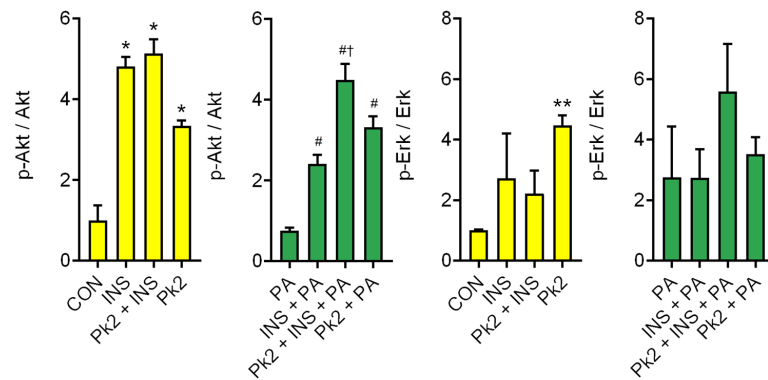
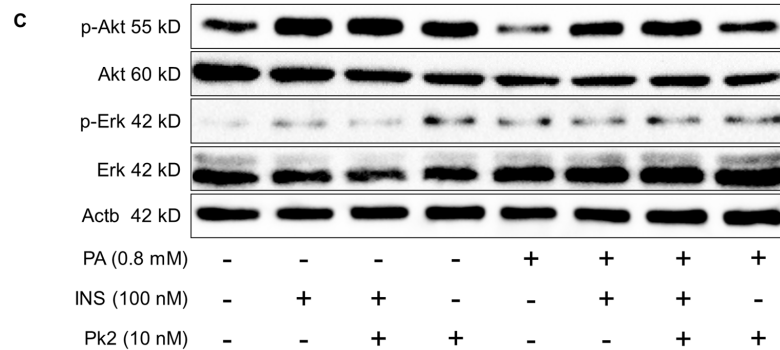


**Figure 4. Effect of Prokr1 activation on the PI3K/Akt signaling pathway in myotubes derived from C2C12 cells and satellite cells**

**(A, B)** Signaling pathways in C2C12 cells-derived myotubes. **A.** Protein levels of phosphorylated Akt (p-Akt), total Akt (Akt), phosphorylated Erk (p-Erk), and total Erk (Erk) in myotubes with different combination of palmitate (PA), insulin (INS) and Pk2 are depicted. Bars indicate mean  $\pm$  SEM of relative levels of p-Akt and p-Erk. \* $p < 0.05$ , \*\* $p < 0.01$ , \*\*\* $p < 0.001$  vs. vehicle control (CON). # $p < 0.05$ , ## $p < 0.01$  vs. PA. † $p < 0.05$  vs. PA + INS. N = 3. **B.** Effect of signaling inhibitors in C2C12 cells-derived myotubes. Protein levels of p-Akt, Akt, p-Erk, and Erk under insulin sensitive condition with U73343 (PLC $\beta$  inhibitor), Wortmannin (WM, PI3K inhibitor) or U0126 (Erk1/2 inhibitor) are qualitatively and quantitatively measured. \* $p < 0.05$ , \*\* $p < 0.01$  vs. CON. Bars indicate mean  $\pm$  SEM of relative levels of p-Akt and p-Erk. N = 3.

**(C, D)** Signaling pathways in satellite cells-derived myotubes. **C.** Protein levels of PI3K/Akt and MAPK/Erk signaling molecules in myotubes with combinatory treatment of PA, INS and Pk2 are depicted. Bars indicate mean  $\pm$  SEM of relative levels of p-Akt and p-Erk. \* $p < 0.05$ , \*\* $p < 0.01$ , \*\*\* $p < 0.001$  vs. vehicle control (CON). # $p < 0.05$ , ## $p < 0.01$  vs. PA. † $p < 0.05$  vs. PA + INS. N = 3. **D.** Effect of signaling inhibitors in satellite cells-derived myotubes. Protein levels of PI3K/Akt and MAPK/Erk signaling molecules under insulin sensitive condition with various signaling inhibitors are qualitatively and quantitatively measured. \* $p < 0.05$ , \*\* $p < 0.01$  vs. CON. Bars indicate mean  $\pm$  SEM of relative levels of p-Akt and p-Erk. N = 3.



## **5. Prokr1 activation induces insulin-stimulated Glut4 translocation in insulin-resistant C2C12 and satellite myotubes**

Insulin stimulation is well known to cause Glucose transporter type 4 (Glut4) translocation to the cell membrane and thus facilitates glucose uptake in the skeletal muscle [51], [52], [53].

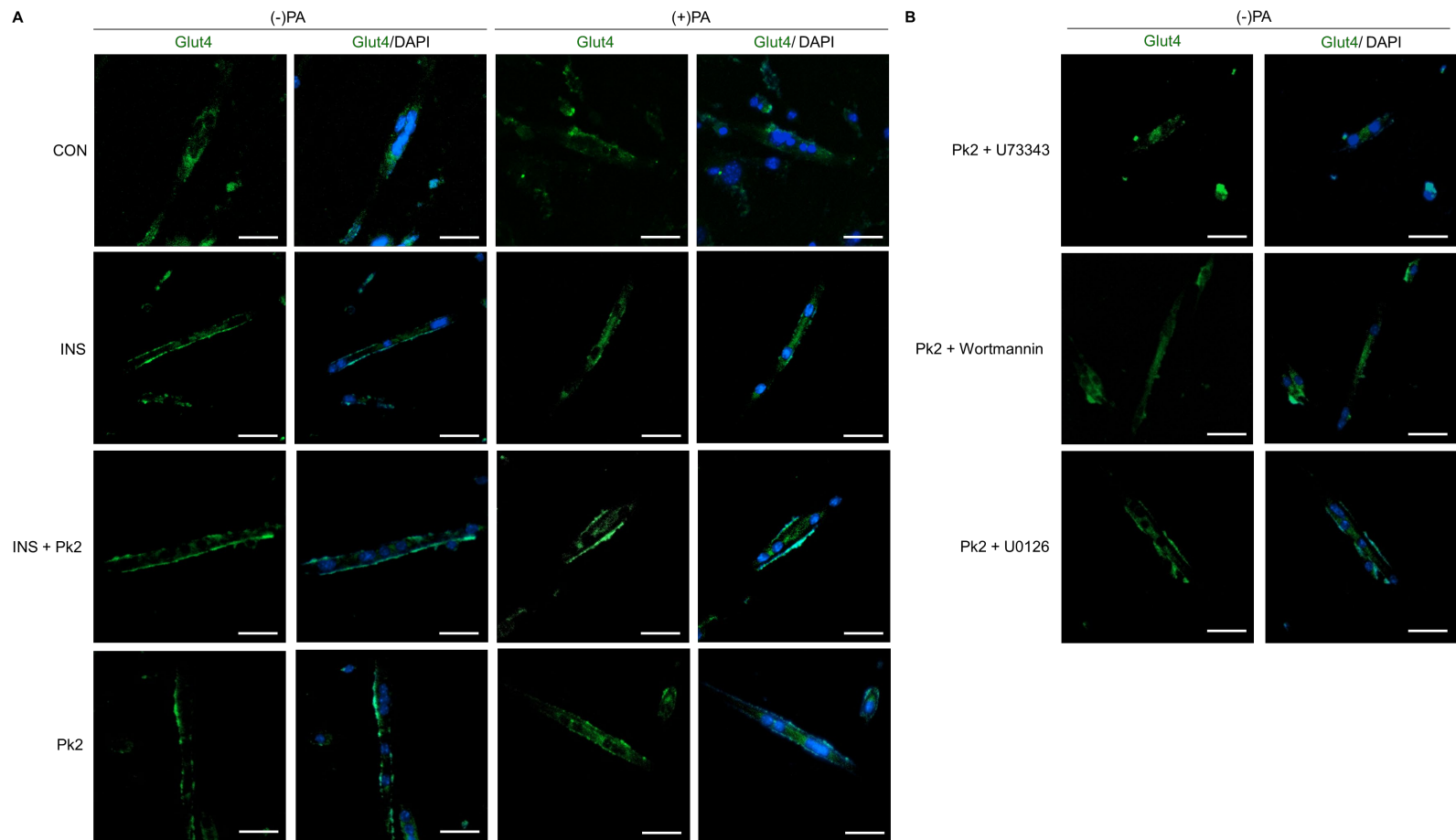
To understand whether PI3K/Akt signaling activated by Prokr1 would increase Glut4 translocation, we examined the Glut4 translocation in myotubes derived from C2C12 and satellite cells.

In insulin sensitive satellite myotubes, Glut4 proteins were concentrated in the cytosol around the nucleus and insulin induced Glut4 translocation to the cell membrane. In palmitate induced insulin-resistant satellite myotubes, insulin had little effect on Glut4 translocation to the membrane. However, cotreatment with Pk2 markedly enhanced the insulin-stimulated Glut4 translocation, and this effect was attenuated in the presence of PLC $\beta$  inhibitor or PI3K inhibitor but not Erk inhibitor (Fig. 5A and B).

In C2C12 myotubes in insulin sensitive, plasma membrane Glut4 as increased by ~5-fold after acute insulin stimulation. Compared to insulin sensitive myotubes, insulin resistant myotubes reduced insulin-induced plasma membrane Glut4 by about 80% in C2C12 myotubes, which could be enhance by Pk2 treatment. In addition, the phosphorylation of Glut4 translocation was remarkably increased by ~ 5-fold with treated Pk2 in both insulin sensitive myotubes and insulin resistant myotube. These effects of

Pk2 on expression of phosphorylated Glut4 translocation was abolished in the presence of either PLC $\beta$  inhibitor U73343 or PI3K inhibitor or Erk inhibitor U0126. (Fig. 5C, D).

These findings suggest that activation of Prokr1 by Pk2 treatment would improve insulin resistance through enhanced translocation of Glut4 through PLC $\beta$ /PI3K/Akt signaling pathway in C2C12 and satellite myotubes.



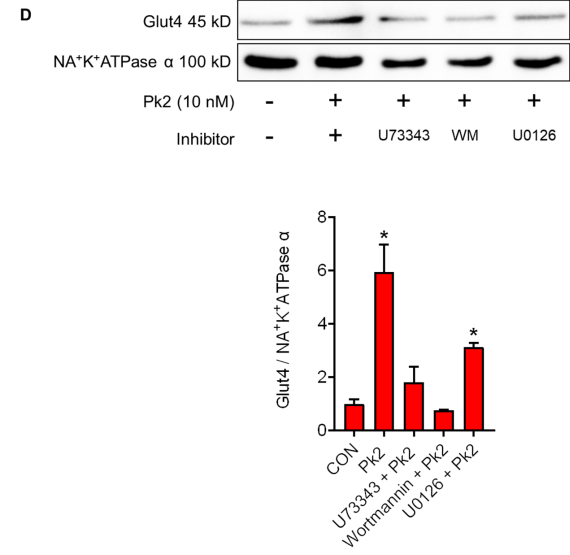
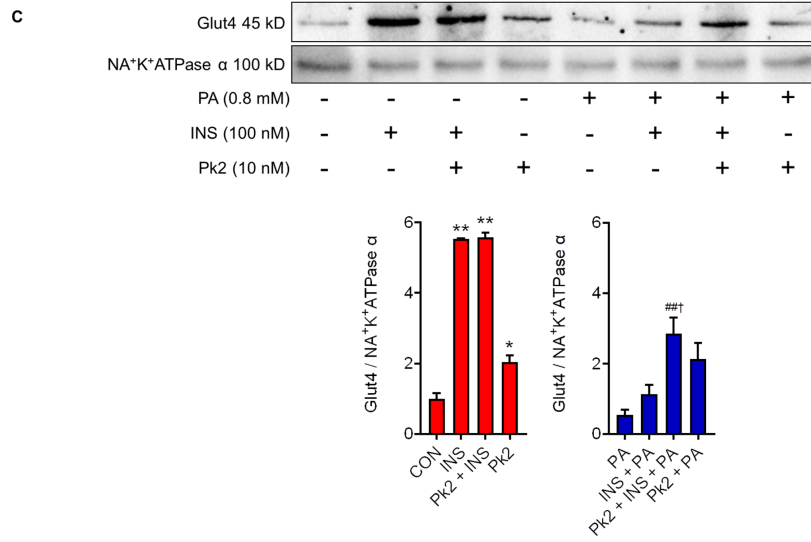


**Figure 5. Prokr1 activation induces insulin-stimulated Glut4 translocation in insulin-resistant C2C12 and satellite myotubes.**

**(A, B)** **A.** Glut4 translocation in insulin sensitive or insulin resistance condition with different combination of treatment of vehicle (CON), insulin (INS) and Pk2 in satellite myotubes is depicted. **B.** Effect of PLC $\beta$  inhibitor (U73343), PI3K inhibitor (Wortmannin; WM) or Erk inhibitor (U0126) on Pk2-induced Glut4 translocation is depicted. The green fluorescence indicates Glut4. Nuclei in all groups are stained in blue with DAPI. Scale bars = 100  $\mu$ m.

**(C, D)** **C.** Plasma membrane-specific Glut4 protein in insulin sensitive or insulin resistance condition with different combination of treatment of INS and Pk2 in C2C12 myotubes is qualitatively and quantitatively measured. **D.** Effect of PLC $\beta$  inhibitor, PI3K inhibitor, or Erk inhibitor on Pk2-induced Glut4 translocation is qualitatively and quantitatively measured. Glut4 translocation level on plasma membrane is normalized with that of Na<sup>+</sup>/K<sup>+</sup>-ATPase. \* $p$  < 0.05 and \*\* $p$  < 0.01 vs. vehicle; # $p$  < 0.05 vs. PA; † $p$  < 0.05 vs. PA + INS. N = 3.

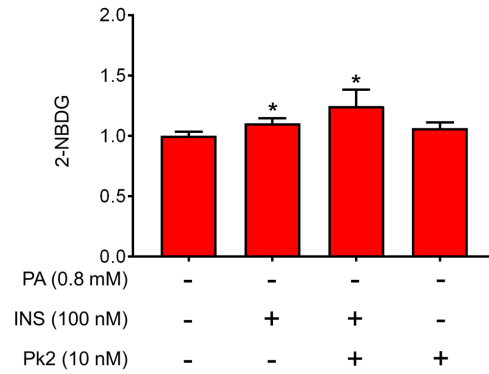
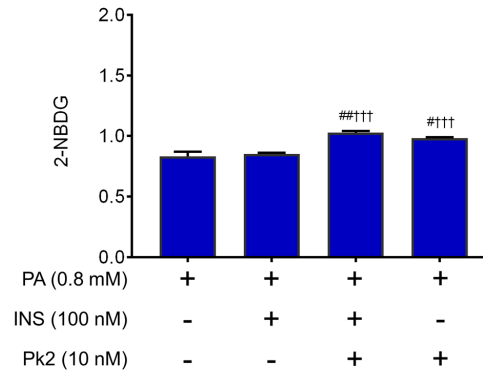
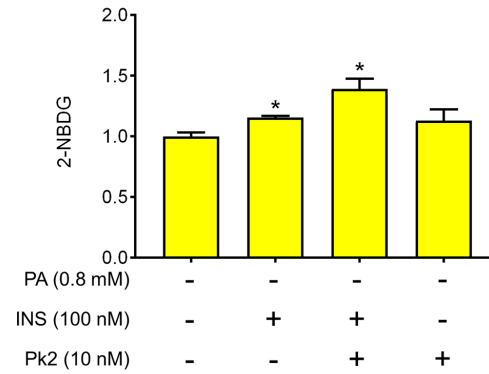
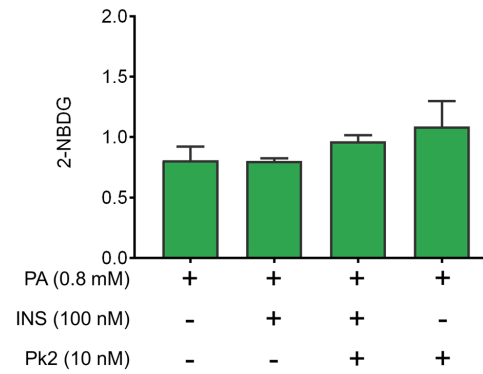
## **6. Effect of Prokr1 activation on insulin-stimulated glucose uptake in myotubes derived from C2C12 cells and satellite cells**

To evaluate whether increased Glut4 translocation through Prokr1 activation would enhance glucose uptake in myotubes derived from C2C12 cells and satellite cells, we examined glucose uptake under insulin sensitive or resistance condition with 2-NBDG, a fluorescence-labeled glucose analogue with different combination of insulin and Pk2 treatment (Fig. 6).

Glucose uptake was significantly improved (approx. 1.2-fold,  $p < 0.05$ ) by insulin treatment in C2C12 cells-derived myotubes under insulin sensitive condition. Co-treatment of Pk2 with insulin increased (approx. 1.3-fold,  $p < 0.05$ ) glucose uptake in C2C12 cells-derived myotubes in insulin sensitive myotubes (Fig. 6A). In contrast, palmitate-induced insulin resistant myotubes showed unchanged levels of glucose uptake by insulin treatment, which were about 80% of insulin sensitive condition in C2C12 cells-derived myotubes. However, co-treatment of Pk2 with insulin ameliorated (approx. 1.3-fold,  $p < 0.05$ ) glucose uptake. Furthermore, glucose uptake was increased (approx. 1.2-fold,  $p < 0.05$ ) by Pk2 treatment only in insulin resistance condition in C2C12 cells-derived myotubes (Fig. 6B).

In satellite cells-derived myotubes under insulin sensitive condition, glucose uptake was significantly improved (approx. 1.2-fold,  $p < 0.05$ ) by insulin treatment in satellite cells-derived myotubes. Co-treatment of Pk2 with insulin increased (approx. 1.3-fold,  $p < 0.05$ ) glucose uptake in satellite cell-

derived myotubes in insulin sensitive myotubes (Fig. 6C). Under palmitate-induced insulin resistant myotubes showed unchanged levels of glucose uptake by insulin treatment, which were about 80% of those in insulin sensitive condition in satellite cells-derived myotubes. Increased trend of glucose uptake was observed by Pk2 treatment and co-treatment of Pk2 with insulin as well in satellite cell-derived myotubes; nevertheless, there was not significant difference under insulin resistance condition (Fig. 6D). These findings suggest that Prokr1 activation would increase insulin sensitivity, which eventually leads to promotion of glucose uptake in C2C12 and satellite-derived myotubes

**A****B****C****D**



**Figure 6. Effect of Prokr1 activation on insulin-stimulated glucose uptake in myotubes derived from C2C12 cells and satellite cells**

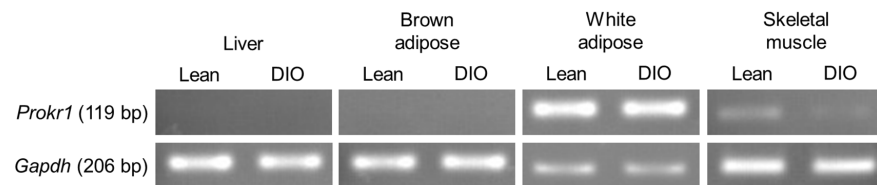
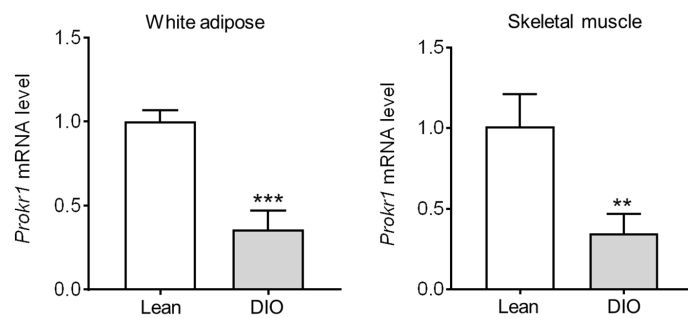
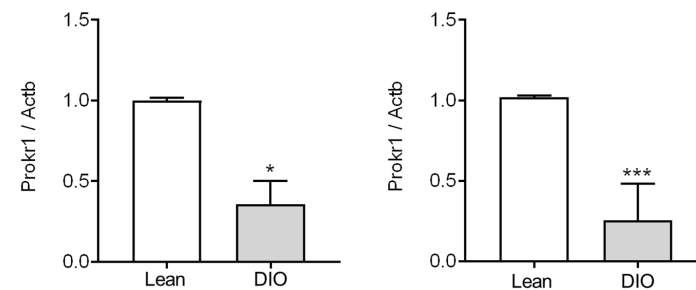
**(A, B)** Glucose uptake in C2C12 cells-derived myotubes under insulin sensitive ((-)PA) or insulin resistance condition ((+)PA). **A.** Glucose uptake levels in myotubes with different combination of vehicle, insulin (INS) and Pk2 under insulin sensitive condition are depicted. Bars indicate mean  $\pm$  SEM of relative levels of 2-NBDG uptake. \* $p < 0.05$  vs. vehicle. **B.**

Glucose uptake levels in myotubes with different combination of vehicle, INS and Pk2 under insulin resistance condition are depicted. Bars indicate mean  $\pm$  SEM of relative levels of 2-NBDG uptake. # $p < 0.05$ , ## $p < 0.01$  vs. vehicle; ††† $p < 0.0001$  vs. vehicle. N = 3.

**(C, D)** Glucose uptake in satellite cells-derived myotubes under insulin sensitive ((-)PA) or insulin resistance condition ((+)PA). **C.** Glucose uptake levels in myotubes with different combination of vehicle, INS and Pk2. Bars indicate mean  $\pm$  SEM of relative levels of 2-NBDG uptake. \* $p < 0.05$  vs. vehicle. **D.** Glucose uptake levels in myotubes with different combination of vehicle, INS and Pk2 under insulin resistance condition. Bars indicate mean  $\pm$  SEM of relative levels of 2-NBDG uptake. N = 3.

## **7. Reduced expression level of Prokr1 in the skeletal muscle of DIO mice**

To understand the *in vivo* relevance of the expression level of Prokr1 in pathogenic condition, we investigated the change of mRNA and protein expression in several tissues of lean and DIO (diet induced obese) mice. The bodyweight and fasting glucose levels of mice showed that DIO mice acquired obese and diabetic phenotype (Table 4). Prokr1 mRNA was detected in white adipose and skeletal muscle, but not in liver and brown adipose (Fig. 7A). In lean mice, the mRNA and protein expression levels of Prokr1 in white adipose tissue and skeletal muscle were higher than DIO mice. Prokr1 mRNA was reduced by approximately 64% in the white adipose and 65% in the skeletal muscle of DIO mice compared to lean mice (Fig. 7B). The Prokr1 protein was also reduced by nearly 65% in the white adipose and 75% in the skeletal muscle of DIO mice compared to lean mice (Fig. 7C). Together, these observations demonstrate that the level of Prokr1 expression would be relevant to metabolic disorders.

**A****B****C**

**Figure 7. Reduced expression level of Prokr1 in the skeletal muscle of DIO mice**

**A.** mRNA expression levels of Prokr1 in various tissues of lean and DIO mice are qualitatively depicted.

**B.** mRNA expression levels of Prokr1 in white adipose and skeletal muscle are quantified between lean and DIO mice. Mean  $\pm$  SD,  $n = 3$ ,  $**p < 0.01$ ,  $***p < 0.001$  vs. lean.

**C.** Protein levels of Prokr1 are qualitatively and quantitatively measured in white adipose and skeletal muscle between lean and DIO mice. Mean  $\pm$  SEM,  $n = 3$ ,  $*p < 0.05$ ,  $***p < 0.001$  vs. lean.

## Discussion

Prokineticin receptor 1 (Prokr1) signaling pathway has been known to play an important role in the central regulation of appetite, the suppression of adipocyte mass, insulin sensitizing in various tissues, cardiac regeneration [34], and kidney development and function [54].

Recently, activation of Prokr1 using non-peptide agonists (IS1 and IS20) have shown that they have an inhibitory effect on cardiac lesion formation and improving cardiac function after myocardial infarction in mice, promoting the proliferation of cardiac progenitor cells and neovascularization [55]. In addition, Prokr1 activation has demonstrated an anti-adipogenic effect in 3T3-L1 adipocytes and adipose specific Prokr1-deficient mice [34].

Therefore, emerging lines of evidence indicate that Prokr1 activation would be effective to control metabolic disorders including Type 2 Diabetes Mellitus (T2DM) not only by increasing the insulin sensitivity in white adipose tissue, delivering insulin to the target organs, but also preventing cardiovascular complications. Skeletal muscle is another major organ responsible for maintaining whole body glucose homeostasis and is responsible for the majority of insulin-stimulated glucose uptake [51].

However, Prokr1 signaling pathway has not been studied in skeletal muscle. If Prokr1 is substantially expressed in skeletal muscles and participates in insulin sensitivity, it could be considered as a potent therapeutic target for T2DM. To validate the metabolic relevance of Prokr1 in skeletal muscle, we

investigated the expression levels of myogenic markers as well as Prokr1 throughout the myogenic differentiation of myoblast C2C12 cells and primary mouse muscular satellite cells. C2C12 cells required 6 days to become mature myotubes. Compared to C2C12 cells, satellite cells appeared to spend 3 days to become mature myotubes. In addition, satellite cells did not require confluency before starting differentiation, which allowed observing single, well-differentiated myotube compared to C2C12-derived myotubes. When comparing differentiation periods and myotube morphology, satellite cells have an advantage compare to C2C12 cell line in several aspects in experiments. During myogenic differentiation, the RNA level of Prokr1 was gradually decreased, but the protein level of Prokr1 was gradually increased. Prokr1 did not seem to be correlated well between mRNA and protein levels during myogenic differentiation. However, it was anticipated that receptor-ligand interaction would be more critical for Prokr1 function; therefore, protein level of Prokr1 was considered more important to determine the substantial expression of Prokr1 instead of mRNA. Prokr1 protein level was increased significantly at myotubes, therefore, most of the pharmacological experiments in this study have been done at the myotube stage.

We analyzed the transcriptome from genetically modified HEK293T cells with the human Prokr1 gene. At first, we expected significantly changes in transcriptional response when human Prokr1 was simply overexpressed in transgenic cell line (HEK293T<sup>Prokr1</sup>) without Prokineticin 2 (Pk2) treatment.

However, no significant changes occurred in HEK293T<sup>Prokr1</sup> without Pk2 treatment. It implies that ligand-mediated receptor activation is essential for transcriptome analysis as well as other pharmacological evaluation especially of G Protein-Coupled Receptors (GPCRs).

In skeletal muscle, glucose transport is primarily regulated by Glucose transporter type 4 (Glut4) [51]. Insulin stimulates glucose uptake by recruiting Glut4 from cytosol to the plasma membrane through a mechanism that is dependent on PI3K/Akt signaling pathway. Insulin resistance seems to be caused by defects in PI3K/Akt signaling pathway, resulting in reduction of Glut4 translocation. Although the exact mechanism of insulin resistance in skeletal muscle is largely unknown, impaired insulin-stimulated glucose uptake by Free Fatty Acid (FFA) is suggested as a putative mechanism of it. Many therapeutic targets have been undergone for repairing insulin resistance by restoring reduced phosphorylation of Akt in skeletal muscle [56] [57].

There are several reports that activation of Prokr1 leads to phosphorylation of Akt as well as Erk in endothelial cells [58], white adipocytes [34] and cardiomyocyte [35]. In accordance with the previous findings on the metabolic effects of Prokr1 in peripheral tissues, we investigated the effect of Prokr1 on glucose transport and its underlying mechanism in the skeletal muscle. First, using myotubes derived from C2C12 cells and primary mouse muscular satellite cells under insulin sensitive and insulin resistance condition, we showed that Prokr1 activation increased phosphorylation of Akt in the presence or absence of insulin. This effect was abolished by

inhibition of PLC $\beta$ /PI3K/Akt and MAPK/Erk signaling pathways using chemical inhibitors. Second, Prokr1 activation promoted translocation of Glut4 in plasma membrane. Third Prokr1 activation enhanced glucose uptake in cultured myotubes. These findings imply a metabolic function of Prokr1 in skeletal muscle that has been unknown previously. In other words, Prokr1 plays an important role in Glut4 translocation, glucose uptake and insulin sensitivity through activation of the PI3K/Akt pathway in skeletal muscle (Fig. 8). Furthermore, current study demonstrates that Prokr1 activation can improve insulin sensitivity, Glut4 translocation and insulin-stimulated glucose uptake in myotubes under both of insulin sensitive and palmitate-induced insulin-resistant conditions. Thus, in addition to previously reported effects of Prokr1 in adipose, endothelial and cardiac tissues, we showed for the first time that activation of Prokr1 would enhance glucose uptake and insulin sensitivity through activation of G<sub>q</sub>-mediated PI3K/Akt signaling in skeletal muscle.

In previous studies, human Prokr1 mRNA levels are reported to be decreased in visceral and subcutaneous adipose tissues in obese people compare to non-obese people [34]. These findings suggest that reduced mRNA level of Prokr1 would be a hallmark of obese patients. We examined the mRNA and protein levels of white fat and skeletal muscle in Diet-Induced Obese (DIO) mice to determine whether the expression levels of Prokr1 in tissues would be correlated with the metabolic phenotype of the mice.



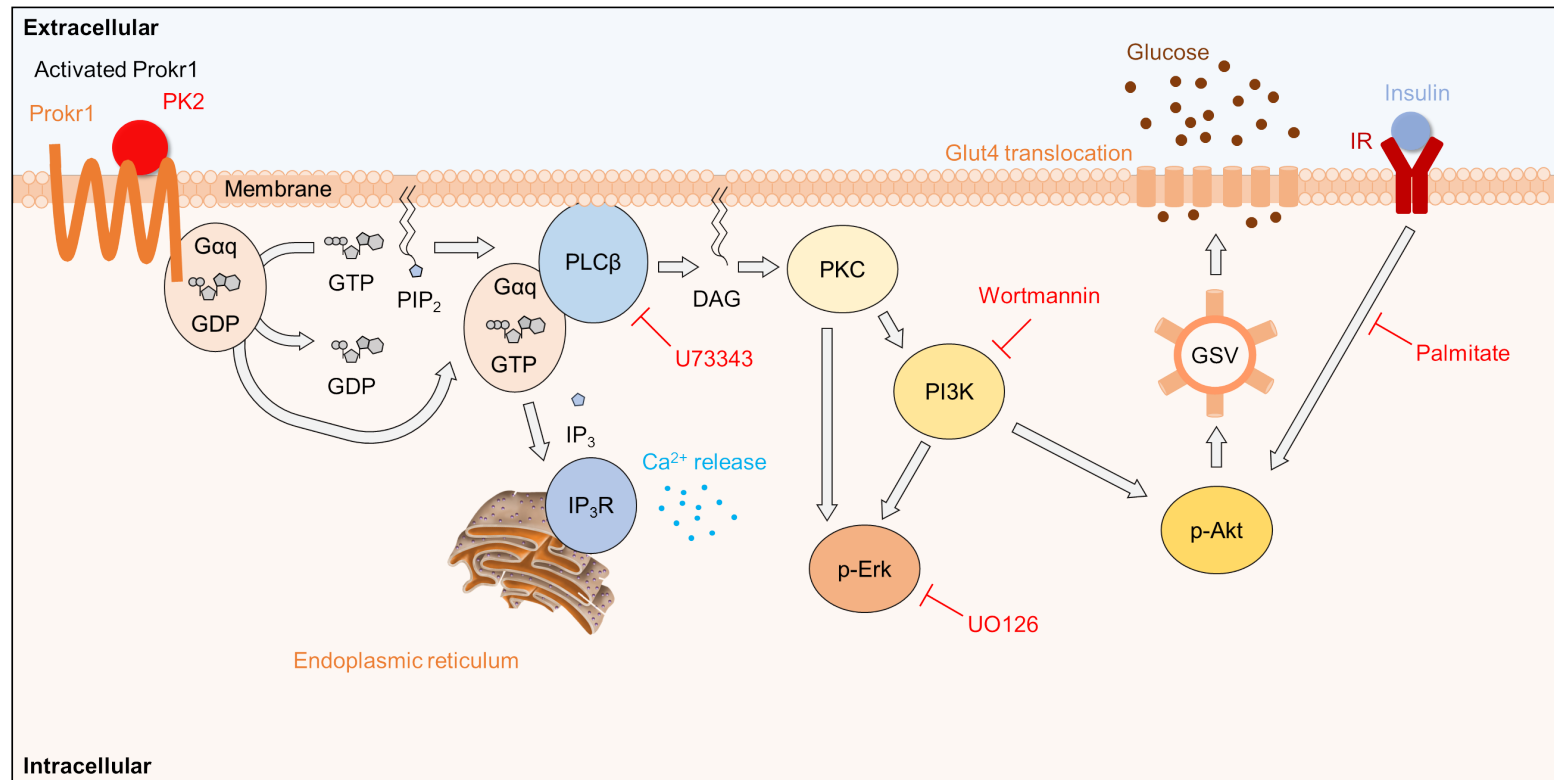


**Figure 8. Schematic summary of Prokr1 signaling pathway for glucose homeostasis in skeletal muscle.**

Compared with lean mice, mRNA and protein levels of Prokr1 in white adipose and skeletal muscle were decreased in DIO mice. Since Prokr1 levels were reduced in DIO mice, it would be anticipated that activation of Prokr1 signaling pathway would contribute for improvement of T2DM.

## **Conclusion**

In summary, this study shows that Prokr1 activation in myotubes derived from C2C12 and satellite cells leads to a significant increase in insulin sensitivity to levels through Prokr1 signaling pathway. Prokr1 would be a potential target for treatment of insulin resistance in T2DM, which can treat not only the underlying treatment but also the substantial benefit of T2DM. As 40% of drugs target GPCRs [59], Prokr1 would be an successful target for treatment or prevention of T2DM. Overall, more studies should be performed to further investigate the potential of Prokr1 to be used to prevent and manage not only insulin resistance but also complication of T2DM. Prokr1 was expected to become a target for new therapies to treat T2DM and complications of T2DM, and it was anticipated to be a new drug that will change the paradigm in the T2DM therapeutic market.

**Table 1. List of primers used in this study**

Gene	Primer	Amplicon	Sequence (5'-3')
Prokr1	forward	119 bp	GCTCTGGTTCGCAGGTTGAA
	reverse		GCAAGGTTGACGACTCCTCT
Prokr2	forward	484 bp	CACACGCCCCACCAAGTAGG
	reverse		TAGCGGGCGAGGGCAGCAATGAA
Human Prokr1	forward	122 bp	CAATTCCAGGACGTTCTTTGCT
	reverse		GCAGTTTCTTGTAGCGGACCA
Myf5	forward	118 bp	AACCCTAACCAGAGACTC
	reverse		CAGACAGGGCTGTTACAT
Myod1	forward	118 bp	CTACAGTGGCGACTCAGA
	reverse		GTAGTAGGCGGTGTCGTA
Pax7	forward	132 bp	TCTCCAAGATTCTGTGCCGAT
	reverse		CGGGGTTCTCTCTCTTATACTCC
Myog	forward	106 bp	GAGACATCCCCCTATTTCTACCA
	reverse		GCTCAGTCCGCTCATAGCC
Mb	forward	108 bp	CTGTTTAAGACTCACCTGAGAC
	reverse		GGTGCAACCATGCTTCTTCA
Myh7	forward	114 bp	ACTGTCAACACTAAGAGGGTCA
	reverse		TTGGATGATTTGATCTTCCAGGG

**(cont'd) Table 1. List of primers used in this study**

Myh2	forward	222 bp	AAGTGACTGTGAAAACAGAAGCA
	reverse		GCAGCCATTTGTAAGGGTTGAC
Gapdh	forward	123 bp	AGGTCGGTGTGAACGGATTTG
	reverse		TGTAGACCATGTAGTTGAGGTCA
GAPDH	forward	82 bp	GAAATCCCATCACCATCT
	reverse		GACTCCACGACGTACTCA

**Table 2. List of Differentially Expressed Genes (DEGs) in Prokr1-activated transgenic HEK293T cells**

Gene symbol	Gene name	Fold change
Up regulated gene		
CGA	glycoprotein hormones, alpha polypeptide	197.584
NR4A2	nuclear receptor subfamily 4, group A, member 2	23.349
NR4A3	nuclear receptor subfamily 4, group A, member 3	17.406
FOSB	FBJ murine osteosarcoma viral oncogene homolog B	15.046
GADD45B	growth arrest and DNA-damage-inducible, beta	14.251
FOSL1	FOS-like antigen 1	13.687
EGR1	early growth response 1	10.895
GPR3	G protein-coupled receptor 3	10.509
JUNB	jun B proto-oncogene	10.220
SV2C	synaptic vesicle glycoprotein 2C	9.483
DUSP1	dual specificity phosphatase 1	9.415
TFPI2	tissue factor pathway inhibitor 2	8.509
INHBA	inhibin beta A	8.250
TNFRSF12A	tumor necrosis factor receptor superfamily, member 12A	6.960
GEM	GTP binding protein overexpressed in skeletal muscle	6.792
ZCCHC12	zinc finger, CCHC domain containing 12	6.791

**(cont'd) Table 2. List of Differentially Expressed Genes (DEGs) in Prokr1-activated transgenic HEK293T cells**

PTGS2	prostaglandin-endoperoxide synthase 2 (prostaglandin G/H synthase and cyclooxygenase)	6.749
TAC1	tachykinin, precursor 1	6.523
OSTN	osteocrin	6.476
SAT1	spermidine/spermine N1-acetyltransferase 1	6.171
NTS	neurotensin	5.870
ATF3	activating transcription factor 3	5.751
SNORA2A	small nucleolar RNA, H/ACA box 2A	5.443
LINC00473	long intergenic non-protein coding RNA 473	5.337
CYR61	cysteine-rich, angiogenic inducer, 61	5.311
CASP9	caspase 9	5.007
NR4A1	nuclear receptor subfamily 4, group A, member 1	4.989
ARC	activity-regulated cytoskeleton-associated protein	4.945
CSRNP1	cysteine-serine-rich nuclear protein 1	4.750
RGCC	regulator of cell cycle	4.571
NEU1	sialidase 1 (lysosomal sialidase)	4.566
CTH	cystathionine gamma-lyase	4.559
GPR50	G protein-coupled receptor 50	4.451
NPPC	natriuretic peptide C	4.276

**(cont'd) Table 2. List of Differentially Expressed Genes (DEGs) in Prokr1-activated transgenic HEK293T cells**

CTGF	connective tissue growth factor	4.269
PCK1	phosphoenolpyruvate carboxykinase 1 (soluble)	4.239
EPHA2	EPH receptor A2	4.005
SLC6A17	solute carrier family 6 (neutral amino acid transporter), member 17	3.984
ADAMTS1	ADAM metalloproteinase with thrombospondin type 1 motif 1	3.862
ELL2	elongation factor, RNA polymerase II, 2	3.834
MAFB	v-maf avian musculoaponeurotic fibrosarcoma oncogene homolog B	3.798
CITED1	Cbp/p300-interacting transactivator, with Glu/Asp rich carboxy-terminal domain, 1	3.788
STEAP1	six transmembrane epithelial antigen of the prostate 1	3.737
SERTAD1	SERTA domain containing 1	3.736
SPRY4	sprouty RTK signaling antagonist 4	3.723
RNF122	ring finger protein 122	3.675
GALR2	galanin receptor 2	3.523
RNU5E-1	RNA, U5E small nuclear 1	3.413
SNORA31	small nucleolar RNA, H/ACA box 31	3.371
PMAIP1	phorbol-12-myristate-13-acetate-induced protein 1	3.337
RNASE3	ribonuclease, RNase A family, 3	3.332
HOMER1	homer scaffolding protein 1	3.329

**(cont'd) Table 2. List of Differentially Expressed Genes (DEGs) in Prokr1-activated transgenic HEK293T cells**

SNORA50C	small nucleolar RNA, H/ACA box 50C	3.315
CHMP1B	charged multivesicular body protein 1B	3.285
TRIB1	tribbles pseudokinase 1	3.227
SNORD14E	small nucleolar RNA, C/D box 14E	3.172
SGMS2	sphingomyelin synthase 2	3.163
VIP	vasoactive intestinal peptide	3.153
LOC105373311	uncharacterized LOC105373311	3.143
CD68	CD68 molecule	3.126
SNORA75	small nucleolar RNA, H/ACA box 75	3.081
NDRG1	N-myc downstream regulated 1	3.037
SCARNA5	small Cajal body-specific RNA 5	3.026
DGKK	diacylglycerol kinase, kappa	3.004
DUSP5	dual specificity phosphatase 5	2.978
GLA	galactosidase, alpha	2.918
CPEB2	cytoplasmic polyadenylation element binding protein 2	2.900
CD55	CD55 molecule, decay accelerating factor for complement (Cromer blood group)	2.894
PVR	poliovirus receptor	2.843
IGKV1-27	immunoglobulin kappa variable 1-27	2.832



**(cont'd) Table 2. List of Differentially Expressed Genes (DEGs) in Prokr1-activated transgenic HEK293T cells**

MIR518D	microRNA 518d	2.830
SNORA33	small nucleolar RNA, H/ACA box 33	2.830
ZDBF2	zinc finger, DBF-type containing 2	2.765
SNORA11	small nucleolar RNA, H/ACA box 11	2.764
MMP10	matrix metalloproteinase 10	2.758
SNORD42A	small nucleolar RNA, C/D box 42A	2.758
ZNF165	zinc finger protein 165	2.747
FOS	FBJ murine osteosarcoma viral oncogene homolog	2.737
LOC105377100	uncharacterized LOC105377100	2.722
MIR519A2	microRNA 519a-2	2.715
MFSD2A	major facilitator superfamily domain containing 2A	2.706
SCARNA23	small Cajal body-specific RNA 23	2.705
KCTD12	potassium channel tetramerization domain containing 12	2.689
NPTX2	neuronal pentraxin II	2.687
RGL1	ral guanine nucleotide dissociation stimulator-like 1	2.682
MMP13	matrix metalloproteinase 13	2.681
PLAUR	plasminogen activator, urokinase receptor	2.656
MIR548AD	microRNA 548ad	2.638

**(cont'd) Table 2. List of Differentially Expressed Genes (DEGs) in Prokr1-activated transgenic HEK293T cells**

ZSCAN12P1	zinc finger and SCAN domain containing 12 pseudogene 1	2.631
TUBB2A	tubulin, beta 2A class IIa	2.626
HIST1H2BG	histone cluster 1, H2bg	2.622
ERRFI1	ERBB receptor feedback inhibitor 1	2.590
SNORD119	small nucleolar RNA, C/D box 119	2.588
CA8	carbonic anhydrase VIII	2.585
MHRT	myosin heavy chain-associated RNA transcript	2.576
TIMP3	TIMP metalloproteinase inhibitor 3	2.575
EMP1	epithelial membrane protein 1	2.568
HIST1H4B	histone cluster 1, H4b	2.565
ROR1-AS1	ROR1 antisense RNA 1	2.548
SNORA13	small nucleolar RNA, H/ACA box 13	2.547
MIR296	microRNA 296	2.542
NEFM	neurofilament, medium polypeptide	2.525
SNORD72	small nucleolar RNA, C/D box 72	2.523
GPAT3	glycerol-3-phosphate acyltransferase 3	2.512
MIR4530	microRNA 4530	2.509
PIM2	Pim-2 proto-oncogene, serine/threonine kinase	2.503

**(cont'd) Table 2. List of Differentially Expressed Genes (DEGs) in Prokr1-activated transgenic HEK293T cells**

GSTTP1	glutathione S-transferase theta pseudogene 1	2.499
MIR378E	microRNA 378e	2.499
CEMIP	cell migration inducing protein, hyaluronan binding	2.496
SIK1	salt-inducible kinase 1	2.490
BTG2	BTG family, member 2	2.480
AREG	amphiregulin	2.480
ACTBL2	actin, beta-like 2	2.474
ETV5	ets variant 5	2.473
IGKV2D-24	immunoglobulin kappa variable 2D-24 (non-functional)	2.470
SNAR-F	small ILF3/NF90-associated RNA F	2.468
MIR516A1	microRNA 516a-1	2.457
LOC105369441	uncharacterized LOC105369441	2.454
HSPA5	heat shock 70kDa protein 5 (glucose-regulated protein, 78kDa)	2.453
C2CD2L	C2CD2-like	2.453
MIR320E	microRNA 320e	2.452
PPEF1	protein phosphatase, EF-hand calcium binding domain 1	2.432
SNORD114-4	small nucleolar RNA, C/D box 114-4	2.432
FAR2P3	fatty acyl-CoA reductase 2 pseudogene 3	2.424

**(cont'd) Table 2. List of Differentially Expressed Genes (DEGs) in Prokr1-activated transgenic HEK293T cells**

SDF2L1	stromal cell-derived factor 2-like 1	2.422
LOC100130849	phosphorylase kinase, gamma 1 (muscle) pseudogene	2.415
CCDC30	coiled-coil domain containing 30	2.410
TPM4	tropomyosin 4	2.403
CLU	clusterin	2.382
SNORD70	small nucleolar RNA, C/D box 70	2.377
HBEGF	heparin-binding EGF-like growth factor	2.376
PLK2	polo-like kinase 2	2.373
PDIA3	protein disulfide isomerase family A member 3	2.367
VTRNA1-3	vault RNA 1-3	2.363
ERVW-1	endogenous retrovirus group W, member 1	2.359
FCGR3B	Fc fragment of IgG, low affinity IIIb, receptor (CD16b)	2.357
VTRNA1-1	vault RNA 1-1	2.348
NFIL3	nuclear factor, interleukin 3 regulated	2.344
IER2	immediate early response 2	2.330
SNORD103A	small nucleolar RNA, C/D box 103A	2.328
SNORD103A	small nucleolar RNA, C/D box 103A	2.328
YRDC	yrdC N(6)-threonylcarbamoyltransferase domain containing	2.315

**(cont'd) Table 2. List of Differentially Expressed Genes (DEGs) in Prokr1-activated transgenic HEK293T cells**

KDM6B	lysine (K)-specific demethylase 6B	2.310
FOSL2	FOS-like antigen 2	2.309
SNORA72	small nucleolar RNA, H/ACA box 72	2.306
MFS12	major facilitator superfamily domain containing 12	2.304
GNG5	guanine nucleotide binding protein (G protein), gamma 5	2.296
SNORD99	small nucleolar RNA, C/D box 99	2.290
ST3GAL5-AS1	ST3GAL5 antisense RNA 1 (head to head)	2.290
CHGB	chromogranin B	2.286
HSPA7	heat shock 70kDa protein 7 (HSP70B)	2.280
LOC100996338	uncharacterized LOC100996338	2.276
ARHGEF3-AS1	ARHGEF3 antisense RNA 1	2.271
MTNR1B	melatonin receptor 1B	2.265
CORO1A	coronin, actin binding protein, 1A	2.264
GPRC5A	G protein-coupled receptor, class C, group 5, member A	2.264
VTRNA1-2	vault RNA 1-2	2.256
SDC4	syndecan 4	2.252
NRARP	NOTCH-regulated ankyrin repeat protein	2.239
SNORA71B	small nucleolar RNA, H/ACA box 71B	2.235

**(cont'd) Table 2. List of Differentially Expressed Genes (DEGs) in Prokr1-activated transgenic HEK293T cells**

MT1CP	metallothionein 1C, pseudogene	2.232
GSTA3	glutathione S-transferase alpha 3	2.228
LOC729732	uncharacterized LOC729732	2.220
RHEBL1	Ras homolog enriched in brain like 1	2.217
JUND	jun D proto-oncogene	2.216
SLCO5A1	solute carrier organic anion transporter family, member 5A1	2.211
SCARNA10	small Cajal body-specific RNA 10	2.211
POM121L9P	POM121 transmembrane nucleoporin-like 9, pseudogene	2.210
MANF	mesencephalic astrocyte-derived neurotrophic factor	2.208
SNORD60	small nucleolar RNA, C/D box 60	2.207
GS1-259H13.2	transmembrane protein 225-like	2.204
BAGE2	B melanoma antigen family, member 2	2.203
LONRF3	LON peptidase N-terminal domain and ring finger 3	2.199
SNORA24	small nucleolar RNA, H/ACA box 24	2.198
LOC105370862	uncharacterized LOC105370862	2.197
NFKB2	nuclear factor of kappa light polypeptide gene enhancer in B-cells 2 (p49/p100)	2.196
MIR320B1	microRNA 320b-1	2.192
SNORD115-45	small nucleolar RNA, C/D box 115-45	2.189

**(cont'd) Table 2. List of Differentially Expressed Genes (DEGs) in Prokr1-activated transgenic HEK293T cells**

LOC105373547	uncharacterized LOC105373547	2.188
C17orf96	chromosome 17 open reading frame 96	2.187
IL6R	interleukin 6 receptor	2.185
JUN	jun proto-oncogene	2.172
NCF1	neutrophil cytosolic factor 1	2.169
RELT	RELT tumor necrosis factor receptor	2.168
SGK1	serum/glucocorticoid regulated kinase 1	2.167
SNORD66	small nucleolar RNA, C/D box 66	2.166
GFPT2	glutamine-fructose-6-phosphate transaminase 2	2.161
KCTD13	potassium channel tetramerization domain containing 13	2.161
GABRQ	gamma-aminobutyric acid (GABA) A receptor, theta	2.150
PNP	purine nucleoside phosphorylase	2.150
DNAJC3	DnaJ (Hsp40) homolog, subfamily C, member 3	2.149
TUBB6	tubulin, beta 6 class V	2.146
VASN	vasorin	2.142
WDR47	WD repeat domain 47	2.142
GCH1	GTP cyclohydrolase 1	2.140
ZFP36L2	ZFP36 ring finger protein-like 2	2.139

**(cont'd) Table 2. List of Differentially Expressed Genes (DEGs) in Prokr1-activated transgenic HEK293T cells**

CALB2	calbindin 2	2.135
MED27	mediator complex subunit 27	2.134
PNPLA8	patatin-like phospholipase domain containing 8	2.129
C3orf84	chromosome 3 open reading frame 84	2.127
TRAV8-6	T cell receptor alpha variable 8-6	2.122
RGS16	regulator of G-protein signaling 16	2.122
LOC102724530	uncharacterized LOC102724530	2.117
TMED9	transmembrane p24 trafficking protein 9	2.116
SNORD63	small nucleolar RNA, C/D box 63	2.112
SLC19A2	solute carrier family 19 (thiamine transporter), member 2	2.110
VDR	vitamin D (1,25- dihydroxyvitamin D3) receptor	2.109
ERO1B	endoplasmic reticulum oxidoreductase beta	2.104
SNORD59A	small nucleolar RNA, C/D box 59A	2.101
ITPKC	inositol-trisphosphate 3-kinase C	2.098
PDIA4	protein disulfide isomerase family A, member 4	2.096
EN2	engrailed homeobox 2	2.096
HNRNPA3	heterogeneous nuclear ribonucleoprotein A3	2.094
NEFL	neurofilament, light polypeptide	2.094



**(cont'd) Table 2. List of Differentially Expressed Genes (DEGs) in Prokr1-activated transgenic HEK293T cells**

KRTAP19-1	keratin associated protein 19-1	2.091
LOC102723895	uncharacterized LOC102723895	2.090
STX11	syntaxin 11	2.084
HIST3H2A	histone cluster 3, H2a	2.081
MYDGF	myeloid-derived growth factor	2.078
HLA-DRA	major histocompatibility complex, class II, DR alpha	2.077
APOOP5	apolipoprotein O pseudogene 5	2.077
ZSWIM6	zinc finger, SWIM-type containing 6	2.075
FGFRL1	fibroblast growth factor receptor-like 1	2.071
MXD1	MAX dimerization protein 1	2.070
SNORD37	small nucleolar RNA, C/D box 37	2.069
PSG3	pregnancy specific beta-1-glycoprotein 3	2.069
LOC151121	uncharacterized LOC151121	2.068
MIR4653	microRNA 4653	2.065
SNORA23	small nucleolar RNA, H/ACA box 23	2.064
OR2L3	olfactory receptor, family 2, subfamily L, member 3	2.062
NIPAL1	NIPA-like domain containing 1	2.062
AREG	amphiregulin	2.062

**(cont'd) Table 2. List of Differentially Expressed Genes (DEGs) in Prokr1-activated transgenic HEK293T cells**

SNORA54	small nucleolar RNA, H/ACA box 54	2.060
RBP5	retinol binding protein 5, cellular	2.060
LGALS13	lectin, galactoside-binding, soluble, 13	2.060
DUSP8	dual specificity phosphatase 8	2.060
SNORA26	small nucleolar RNA, H/ACA box 26	2.057
IFFO2	intermediate filament family orphan 2	2.055
HERPUD1	homocysteine-inducible, endoplasmic reticulum stress-inducible, ubiquitin-like domain member 1	2.055
SNORA38B	small nucleolar RNA, H/ACA box 38B	2.050
SNORD71	small nucleolar RNA, C/D box 71	2.048
TRAV29DV5	T cell receptor alpha variable 29/delta variable 5 (gene/pseudogene)	2.046
HEXIM1	hexamethylene bis-acetamide inducible 1	2.045
DIRC2	disrupted in renal carcinoma 2	2.045
SNORD16	small nucleolar RNA, C/D box 16	2.041
HSPA1B	heat shock 70kDa protein 1B	2.041
DKK1	dickkopf WNT signaling pathway inhibitor 1	2.040
SNORD92	small nucleolar RNA, C/D box 92	2.039
FKBP2	FK506 binding protein 2	2.032
KRTAP9-7	keratin associated protein 9-7	2.032

**(cont'd) Table 2. List of Differentially Expressed Genes (DEGs) in Prokr1-activated transgenic HEK293T cells**

TMEM2	transmembrane protein 2	2.026
SCARNA7	small Cajal body-specific RNA 7	2.025
LOC105371559	uncharacterized LOC105371559	2.025
LOC105374748	uncharacterized LOC105374748	2.023
INSIG1	insulin induced gene 1	2.023
LOC105378811	uncharacterized LOC105378811	2.022
SLC3A2	solute carrier family 3 (amino acid transporter heavy chain), member 2	2.021
ATP1B3	ATPase, Na <sup>+</sup> /K <sup>+</sup> transporting, beta 3 polypeptide	2.020
RNU11	RNA, U11 small nuclear	2.020
LOC728660	uncharacterized LOC728660	2.014
LOC105369783	uncharacterized LOC105369783	2.014
RRN3P1	RRN3 homolog, RNA polymerase I transcription factor pseudogene 1	2.014
MIR450A1	microRNA 450a-1	2.011
AVPI1	arginine vasopressin-induced 1	2.010
MIR1321	microRNA 1321	2.009
PPP1R15A	protein phosphatase 1, regulatory subunit 15A	2.004
TRAV20	T cell receptor alpha variable 20	2.003
LSR	lipolysis stimulated lipoprotein receptor	2.003

**(cont'd) Table 2. List of Differentially Expressed Genes (DEGs) in Prokr1-activated transgenic HEK293T cells**

FAM83G	family with sequence similarity 83, member G	2.002
Down regulated gene		
SLC16A9	solute carrier family 16, member 9	-2.000
ADAL	adenosine deaminase-like	-2.001
LOC101928026	uncharacterized LOC101928026	-2.001
LOC100653233	uncharacterized LOC100653233	-2.001
IFT88	intraflagellar transport 88	-2.003
FRRS1L	ferric-chelate reductase 1-like	-2.003
LOC101930131	uncharacterized LOC101930131	-2.004
ZXDA	zinc finger, X-linked, duplicated A	-2.006
DHRS3	dehydrogenase/reductase (SDR family) member 3	-2.007
PREX2	phosphatidylinositol-3,4,5-trisphosphate-dependent Rac exchange factor 2	-2.007
LNP1	leukemia NUP98 fusion partner 1	-2.007
KIAA0922	KIAA0922	-2.008
SMAD9	SMAD family member 9	-2.009
PUS7L	pseudouridylate synthase 7-like	-2.010
ZNF283	zinc finger protein 283	-2.010
SCRN1	secernin 1	-2.011
FAAH2	fatty acid amide hydrolase 2	-2.017

**(cont'd) Table 2. List of Differentially Expressed Genes (DEGs) in Prokr1-activated transgenic HEK293T cells**

GSE1	Gse1 coiled-coil protein	-2.017
YTHDC2	YTH domain containing 2	-2.019
SWT1	SWT1 RNA endoribonuclease homolog	-2.020
ARHGEF26	Rho guanine nucleotide exchange factor 26	-2.020
PCDH7	protocadherin 7	-2.022
LOC105371220	uncharacterized LOC105371220	-2.025
CABLES1	Cdk5 and Abl enzyme substrate 1	-2.027
UHRF1BP1	UHRF1 binding protein 1	-2.028
PARP4	poly(ADP-ribose) polymerase family member 4	-2.030
MTMR7	myotubularin related protein 7	-2.031
ATP9A	ATPase, class II, type 9A	-2.032
LOC646778	uncharacterized LOC646778	-2.033
LOC84214	uncharacterized LOC84214	-2.034
SPG11	spastic paraplegia 11 (autosomal recessive)	-2.035
TUG1	taurine up-regulated 1 (non-protein coding)	-2.036
CAMK2D	calcium/calmodulin-dependent protein kinase II delta	-2.039
LINC00476	long intergenic non-protein coding RNA 476	-2.042
ADGRL2	adhesion G protein-coupled receptor L2	-2.042

**(cont'd) Table 2. List of Differentially Expressed Genes (DEGs) in Prokr1-activated transgenic HEK293T cells**

ANKRD10	ankyrin repeat domain 10	-2.044
HOXC9	homeobox C9	-2.049
ZNF876P	zinc finger protein 876, pseudogene	-2.050
CRIPAK	cysteine-rich PAK1 inhibitor	-2.051
RPARP-AS1	RPARP antisense RNA 1	-2.051
BCOR	BCL6 corepressor	-2.052
GUCY1B3	guanylate cyclase 1, soluble, beta 3	-2.052
DIS3L	DIS3 like exosome 3-5 exoribonuclease	-2.053
USP40	ubiquitin specific peptidase 40	-2.053
FOXP1	forkhead box P1	-2.055
NR2F2	nuclear receptor subfamily 2, group F, member 2	-2.055
ZC3H6	zinc finger CCCH-type containing 6	-2.056
ZNF91	zinc finger protein 91	-2.056
ELMOD1	ELMO/CED-12 domain containing 1	-2.056
ELOVL6	ELOVL fatty acid elongase 6	-2.060
ZNF260	zinc finger protein 260	-2.061
RPL23AP32	ribosomal protein L23a pseudogene 32	-2.063
SERPINB4	serpin peptidase inhibitor, clade B (ovalbumin), member 4	-2.063

**(cont'd) Table 2. List of Differentially Expressed Genes (DEGs) in Prokr1-activated transgenic HEK293T cells**

---

FAR2P1	fatty acyl-CoA reductase 2 pseudogene 1	-2.063
IZUMO1R	IZUMO1 receptor, JUNO	-2.063
LOC101927999	putative uncharacterized protein encoded by LINC00174	-2.064
FMO4	flavin containing monooxygenase 4	-2.065
CSH2	chorionic somatomammotropin hormone 2	-2.066
FOXP2	forkhead box P2	-2.066
EML5	echinoderm microtubule associated protein like 5	-2.066
DIXDC1	DIX domain containing 1	-2.067
ZBED8	zinc finger, BED-type containing 8	-2.068
C1orf21	chromosome 1 open reading frame 21	-2.069
RUNX1T1	runt-related transcription factor 1; translocated to, 1 (cyclin D-related)	-2.069
ETNPPL	ethanolamine-phosphate phospho-lyase	-2.071
NIPA1	non imprinted in Prader-Willi/Angelman syndrome 1	-2.072
NNT-AS1	NNT antisense RNA 1	-2.075
BRCA2	breast cancer 2, early onset	-2.076
PPM1H	protein phosphatase, Mg <sup>2+</sup> /Mn <sup>2+</sup> dependent, 1H	-2.081
MLLT3	myeloid/lymphoid or mixed-lineage leukemia; translocated to, 3	-2.082
KIAA1107	KIAA1107	-2.083

---

**(cont'd) Table 2. List of Differentially Expressed Genes (DEGs) in Prokr1-activated transgenic HEK293T cells**

LOC157860	uncharacterized LOC157860	-2.083
MSANTD1	Myb/SANT-like DNA-binding domain containing 1	-2.085
SPRR2F	small proline-rich protein 2F	-2.085
HOTAIR	HOX transcript antisense RNA	-2.086
N4BP2L2-IT2	N4BPL2 intronic transcript 2	-2.086
LOC105370309	uncharacterized LOC105370309	-2.088
C19orf54	chromosome 19 open reading frame 54	-2.090
MIR3926-2	microRNA 3926-2	-2.090
VPS39	vacuolar protein sorting 39 homolog (S. cerevisiae)	-2.091
EMC3-AS1	EMC3 antisense RNA 1	-2.094
LOC100996713	uncharacterized LOC100996713	-2.094
TTC30B	tetratricopeptide repeat domain 30B	-2.095
RMI1	RecQ mediated genome instability 1	-2.097
TET1	tet methylcytosine dioxygenase 1	-2.097
ZADH2	zinc binding alcohol dehydrogenase domain containing 2	-2.098
ARHGEF6	Rac/Cdc42 guanine nucleotide exchange factor 6	-2.100
LOC101926908	uncharacterized LOC101926908	-2.100
MEIS2	Meis homeobox 2	-2.102



**(cont'd) Table 2. List of Differentially Expressed Genes (DEGs) in Prokr1-activated transgenic HEK293T cells**

DLG3	discs, large homolog 3 (Drosophila)	-2.106
MIR16-2	microRNA 16-2	-2.108
ZNF512	zinc finger protein 512	-2.108
PUS10	pseudouridylate synthase 10	-2.108
CDK6	cyclin-dependent kinase 6	-2.111
RPGRIP1L	RPGRIP1-like	-2.113
LOC105374357	uncharacterized LOC105374357	-2.117
LOC105373341	uncharacterized LOC105373341	-2.122
MIR1302-5	microRNA 1302-5	-2.123
SLC7A2	solute carrier family 7 (cationic amino acid transporter, y <sup>+</sup> system), member 2	-2.126
KREMEN1	kringle containing transmembrane protein 1	-2.127
SLC24A1	solute carrier family 24 (sodium/potassium/calcium exchanger), member 1	-2.127
GREB1L	growth regulation by estrogen in breast cancer-like	-2.129
LOC101928868	atherin-like	-2.129
PMS1	PMS1 homolog 1, mismatch repair system component	-2.130
SMAD6	SMAD family member 6	-2.135
MIR573	microRNA 573	-2.144
PMS2P9	PMS1 homolog 2, mismatch repair system component pseudogene 9	-2.145

**(cont'd) Table 2. List of Differentially Expressed Genes (DEGs) in Prokr1-activated transgenic HEK293T cells**

KRTAP10-4	keratin associated protein 10-4	-2.145
MAOA	monoamine oxidase A	-2.146
LOC105377755	uncharacterized LOC105377755	-2.147
SPRR1B	small proline-rich protein 1B	-2.147
PDE5A	phosphodiesterase 5A, cGMP-specific	-2.149
NLRX1	NLR family member X1	-2.156
PRAMEF6	PRAME family member 6	-2.158
KIF13A	kinesin family member 13A	-2.159
ZFP62	ZFP62 zinc finger protein	-2.161
MAML2	mastermind-like transcriptional coactivator 2	-2.163
MAP4K1	mitogen-activated protein kinase kinase kinase kinase 1	-2.166
GIN1	gypsy retrotransposon integrase 1	-2.167
IGBP1P1	immunoglobulin (CD79A) binding protein 1 pseudogene 1	-2.169
PLXDC2	plexin domain containing 2	-2.171
DKFZP586I1420	uncharacterized protein DKFZp586I1420	-2.173
ZIC2	Zic family member 2	-2.173
TOMM20L	translocase of outer mitochondrial membrane 20 homolog (yeast)-like	-2.177
ZFHX4	zinc finger homeobox 4	-2.177

**(cont'd) Table 2. List of Differentially Expressed Genes (DEGs) in Prokr1-activated transgenic HEK293T cells**

FAM86C2P	family with sequence similarity 86, member A pseudogene	-2.179
C17orf58	chromosome 17 open reading frame 58	-2.181
KCTD19	potassium channel tetramerization domain containing 19	-2.181
FAT4	FAT atypical cadherin 4	-2.182
LOC101927016	keratin-associated protein 21-1-like	-2.182
CIT	citron rho-interacting serine/threonine kinase	-2.183
ATP2B4	ATPase, Ca <sup>++</sup> transporting, plasma membrane 4	-2.186
QIQN5815	uncharacterized LOC100129033	-2.187
ZSWIM7	zinc finger, SWIM-type containing 7	-2.187
CROT	carnitine O-octanoyltransferase	-2.187
HNRNPA1L2	heterogeneous nuclear ribonucleoprotein A1-like 2	-2.194
NYNRIN	NYN domain and retroviral integrase containing	-2.197
KIF5A	kinesin family member 5A	-2.199
MIR4279	microRNA 4279	-2.200
ADGRB3	adhesion G protein-coupled receptor B3	-2.215
CEP290	centrosomal protein 290kDa	-2.215
LOC105373997	uncharacterized LOC105373997	-2.218
CCDC121	coiled-coil domain containing 121	-2.219

**(cont'd) Table 2. List of Differentially Expressed Genes (DEGs) in Prokr1-activated transgenic HEK293T cells**

LOC100288842	UDP-GlcNAc:betaGal beta-1,3-N-acetylglucosaminyltransferase 5 pseudogene	-2.222
LOC105374374	uncharacterized LOC105374374	-2.223
EPB41L4A	erythrocyte membrane protein band 4.1 like 4A	-2.224
GPAM	glycerol-3-phosphate acyltransferase, mitochondrial	-2.225
PGGT1B	protein geranylgeranyltransferase type I, beta subunit	-2.226
RNF213	ring finger protein 213	-2.226
SIM1	single-minded family bHLH transcription factor 1	-2.230
ZNF618	zinc finger protein 618	-2.231
FAM35DP	family with sequence similarity 35, member A pseudogene	-2.240
SNORD101	small nucleolar RNA, C/D box 101	-2.241
CAMKK1	calcium/calmodulin-dependent protein kinase kinase 1, alpha	-2.241
PBX1	pre-B-cell leukemia homeobox 1	-2.243
PCF11	PCF11 cleavage and polyadenylation factor subunit	-2.247
ZNF766	zinc finger protein 766	-2.248
LRRC34	leucine rich repeat containing 34	-2.251
ZSCAN30	zinc finger and SCAN domain containing 30	-2.251
CDK14	cyclin-dependent kinase 14	-2.259
GRB14	growth factor receptor bound protein 14	-2.267

**(cont'd) Table 2. List of Differentially Expressed Genes (DEGs) in Prokr1-activated transgenic HEK293T cells**

GCSHP3	glycine cleavage system protein H (aminomethyl carrier) pseudogene 3	-2.268
LOC101928906	uncharacterized LOC101928906	-2.272
METTL7B	methyltransferase like 7B	-2.277
ZNF585B	zinc finger protein 585B	-2.277
CASC9	cancer susceptibility candidate 9 (non-protein coding)	-2.278
TRMT1L	tRNA methyltransferase 1 like	-2.281
C15orf41	chromosome 15 open reading frame 41	-2.287
DST	dystonin	-2.288
HOXB3	homeobox B3	-2.291
LOC105377538	uncharacterized LOC105377538	-2.291
LYPD1	LY6/PLAUR domain containing 1	-2.300
DOCK11	dedicator of cytokinesis 11	-2.307
EDA2R	ectodysplasin A2 receptor	-2.309
RAD51D	RAD51 paralog D	-2.313
ZNF462	zinc finger protein 462	-2.314
LOC100287934	uncharacterized LOC100287934	-2.321
SULT1C4	sulfotransferase family 1C member 4	-2.325
ZNF19	zinc finger protein 19	-2.326

**(cont'd) Table 2. List of Differentially Expressed Genes (DEGs) in Prokr1-activated transgenic HEK293T cells**

KAT6B	K(lysine) acetyltransferase 6B	-2.327
DPY19L2	dpy-19-like 2 (C. elegans)	-2.330
LRP2	LDL receptor related protein 2	-2.331
SAMD12	sterile alpha motif domain containing 12	-2.331
ZNF429	zinc finger protein 429	-2.336
LOC105372441	uncharacterized LOC105372441	-2.337
LIG3	ligase III, DNA, ATP-dependent	-2.338
OLMALINC	oligodendrocyte maturation-associated long intergenic non-coding RNA	-2.344
ALOX12-AS1	ALOX12 antisense RNA 1	-2.344
IKBKE	inhibitor of kappa light polypeptide gene enhancer in B-cells, kinase epsilon	-2.345
LOC102725021	uncharacterized LOC102725021	-2.346
RHOBTB1	Rho-related BTB domain containing 1	-2.350
KNTC1	kinetochore associated 1	-2.357
NDNF	neuron-derived neurotrophic factor	-2.357
MIR499B	microRNA 499b	-2.359
ANKEF1	ankyrin repeat and EF-hand domain containing 1	-2.360
AMOT	angiomin	-2.362
LRRC37B	leucine rich repeat containing 37B	-2.365

**(cont'd) Table 2. List of Differentially Expressed Genes (DEGs) in Prokr1-activated transgenic HEK293T cells**

PTPN14	protein tyrosine phosphatase, non-receptor type 14	-2.367
KLHL14	kelch-like family member 14	-2.368
YAP1	Yes-associated protein 1	-2.370
METTL7A	methyltransferase like 7A	-2.375
FOXF2	forkhead box F2	-2.378
WDHD1	WD repeat and HMG-box DNA binding protein 1	-2.381
ZSCAN23	zinc finger and SCAN domain containing 23	-2.386
UNC5C	unc-5 netrin receptor C	-2.387
KRBA2	KRAB-A domain containing 2	-2.389
HLA-F-AS1	HLA-F antisense RNA 1	-2.396
ZNF362	zinc finger protein 362	-2.399
LINC00491	long intergenic non-protein coding RNA 491	-2.403
MBOAT1	membrane bound O-acyltransferase domain containing 1	-2.407
ARHGAP28	Rho GTPase activating protein 28	-2.417
POGZ	pogo transposable element with ZNF domain	-2.428
MIR4738	microRNA 4738	-2.430
GPX8	glutathione peroxidase 8 (putative)	-2.436
SLC9A7P1	solute carrier family 9, subfamily A (NHE7, cation proton antiporter 7), member 7 pseudogene 1	-2.443

**(cont'd) Table 2. List of Differentially Expressed Genes (DEGs) in Prokr1-activated transgenic HEK293T cells**

---

COLEC12	collectin sub-family member 12	-2.449
ADAM1A	ADAM metallopeptidase domain 1A (pseudogene)	-2.453
HOXD3	homeobox D3	-2.455
SIK3-IT1	SIK3 intronic transcript 1	-2.459
TBL1XR1	transducin (beta)-like 1 X-linked receptor 1	-2.471
SLC44A5	solute carrier family 44, member 5	-2.473
TGFB3	transforming growth factor beta receptor III	-2.474
TNIK	TRAF2 and NCK interacting kinase	-2.481
DPH5	diphthamide biosynthesis 5	-2.482
ASXL3	additional sex combs like transcriptional regulator 3	-2.494
KLF12	Kruppel-like factor 12	-2.494
PMS2	PMS1 homolog 2, mismatch repair system component	-2.499
USP28	ubiquitin specific peptidase 28	-2.500
TPTE2P1	transmembrane phosphoinositide 3-phosphatase and tensin homolog 2 pseudogene 1	-2.503
ITGA8	integrin alpha 8	-2.506
HOXB5	homeobox B5	-2.510
CYP4F2	cytochrome P450, family 4, subfamily F, polypeptide 2	-2.511
CYP4V2	cytochrome P450, family 4, subfamily V, polypeptide 2	-2.516

---



**(cont'd) Table 2. List of Differentially Expressed Genes (DEGs) in Prokr1-activated transgenic HEK293T cells**

ZNF611	zinc finger protein 611	-2.516
FLRT3	fibronectin leucine rich transmembrane protein 3	-2.521
TMCC1-AS1	TMCC1 antisense RNA 1 (head to head)	-2.546
EPHA7	EPH receptor A7	-2.551
ZNF827	zinc finger protein 827	-2.558
LOC440173	uncharacterized LOC440173	-2.558
MBOAT2	membrane bound O-acyltransferase domain containing 2	-2.564
KIT	v-kit Hardy-Zuckerman 4 feline sarcoma viral oncogene homolog	-2.565
LINC00265	long intergenic non-protein coding RNA 265	-2.576
MET	MET proto-oncogene, receptor tyrosine kinase	-2.580
BACE1-AS	BACE1 antisense RNA	-2.580
SCN9A	sodium channel, voltage gated, type IX alpha subunit	-2.591
DTNA	dystrobrevin, alpha	-2.598
SULF2	sulfatase 2	-2.607
DDIT4	DNA damage inducible transcript 4	-2.609
WNT5A	wingless-type MMTV integration site family, member 5A	-2.610
FENDRR	FOXF1 adjacent non-coding developmental regulatory RNA	-2.611
SEMA3D	sema domain, immunoglobulin domain (Ig), short basic domain, secreted, (semaphorin) 3D	-2.626

**(cont'd) Table 2. List of Differentially Expressed Genes (DEGs) in Prokr1-activated transgenic HEK293T cells**

TTF2	transcription termination factor, RNA polymerase II	-2.639
CTPS2	CTP synthase 2	-2.644
LINC00342	long intergenic non-protein coding RNA 342	-2.650
ZMYM3	zinc finger, MYM-type 3	-2.654
DUSP19	dual specificity phosphatase 19	-2.664
KBTBD7	kelch repeat and BTB (POZ) domain containing 7	-2.671
NFIA	nuclear factor I/A	-2.674
LOC105379521	uncharacterized LOC105379521	-2.685
RARB	retinoic acid receptor, beta	-2.686
PRTG	protogenin	-2.691
ITGA2	integrin, alpha 2 (CD49B, alpha 2 subunit of VLA-2 receptor)	-2.693
DZIP3	DAZ interacting zinc finger protein 3	-2.701
DAPK1	death-associated protein kinase 1	-2.713
PRAMEF11	PRAME family member 11	-2.720
ZNF708	zinc finger protein 708	-2.729
MAP3K5	mitogen-activated protein kinase kinase kinase 5	-2.734
BRINP3	bone morphogenetic protein/retinoic acid inducible neural-specific 3	-2.755
NUTM2B-AS1	NUTM2B antisense RNA 1	-2.755

**(cont'd) Table 2. List of Differentially Expressed Genes (DEGs) in Prokr1-activated transgenic HEK293T cells**

---

C9orf3	chromosome 9 open reading frame 3	-2.785
IQGAP2	IQ motif containing GTPase activating protein 2	-2.830
NUAK1	NUAK family, SNF1-like kinase, 1	-2.831
ZNF608	zinc finger protein 608	-2.858
EHHADH	enoyl-CoA, hydratase/3-hydroxyacyl CoA dehydrogenase	-2.881
HOXA2	homeobox A2	-2.882
SERTAD4	SERTA domain containing 4	-2.893
LINC01351	long intergenic non-protein coding RNA 1351	-2.894
CCDC113	coiled-coil domain containing 113	-2.900
PLCH1	phospholipase C, eta 1	-2.938
GUCY1A3	guanylate cyclase 1, soluble, alpha 3	-2.950
HOXA13	homeobox A13	-2.954
ZFP14	ZFP14 zinc finger protein	-2.977
TEX15	testis expressed 15	-3.012
LOC644794	uncharacterized LOC644794	-3.035
NR3C2	nuclear receptor subfamily 3, group C, member 2	-3.036
HOXA11-AS	HOXA11 antisense RNA	-3.056
NFIB	nuclear factor I/B	-3.063

---

**(cont'd) Table 2. List of Differentially Expressed Genes (DEGs) in Prokr1-activated transgenic HEK293T cells**

LINC01021	long intergenic non-protein coding RNA 1021	-3.083
LINC00648	long intergenic non-protein coding RNA 648	-3.093
ZNF430	zinc finger protein 430	-3.125
SOD2	superoxide dismutase 2, mitochondrial	-3.144
NRP1	neuropilin 1	-3.152
MECOM	MDS1 and EVI1 complex locus	-3.228
NCOA2	nuclear receptor coactivator 2	-3.277
SEMA3A	sema domain, immunoglobulin domain (Ig), short basic domain, secreted, (semaphorin) 3A	-3.291
VCAN	versican	-3.312
MIR520C	microRNA 520c	-3.328
LOC257396	uncharacterized LOC257396	-3.350
FAM45A	family with sequence similarity 45, member A	-3.370
GPRIN3	GPRIN family member 3	-3.530
TRERF1	transcriptional regulating factor 1	-3.541
DACH1	dachshund family transcription factor 1	-3.872
PLEKHG1	pleckstrin homology domain containing, family G (with RhoGef domain) member 1	-3.973
PLEKHA2	pleckstrin homology domain containing, family A (phosphoinositide binding specific) member 2	-4.110
MIR548AM	microRNA 548am	-4.212

**(cont'd) Table 2. List of Differentially Expressed Genes (DEGs) in Prokr1-activated transgenic HEK293T cells**

FAM83B	family with sequence similarity 83, member B	-4.230
MAP2K6	mitogen-activated protein kinase kinase 6	-4.599
PDIA3P1	protein disulfide isomerase family A member 3 pseudogene 1	-4.738
SLITRK5	SLIT and NTRK-like family, member 5	-5.956

**Table 3. List of Kyoto Encyclopedia of Genes and Genomes (KEGG) pathway-enriched genes**

Gene symbol	Gene name	Fold change	P-value	FDR
1. MAPK signaling pathway				
Up regulated gene				
GADD45B	growth arrest and DNA-damage-inducible, beta	14.25	1.4E-13	2.0E-11
DUSP1	dual specificity phosphatase 1	9.415	1.4E-13	2.0E-11
NR4A1	nuclear receptor subfamily 4, group A, member 1	4.989	1.4E-13	2.0E-11
EPHA2	EPH receptor A2	4.005	1.4E-13	2.0E-11
DUSP5	dual specificity phosphatase 5	2.978	1.4E-13	2.0E-11
FOS	FBJ murine osteosarcoma viral oncogene homolog	2.737	1.4E-13	2.0E-11
AREG	amphiregulin	2.480	1.4E-13	2.0E-11
JUND	jun D proto-oncogene	2.216	1.4E-13	2.0E-11
NFKB2	nuclear factor of kappa light polypeptide gene enhancer in B-cells 2 (p49/p100)	2.196	1.4E-13	2.0E-11
JUN	jun proto-oncogene	2.172	1.4E-13	2.0E-11
AREG	amphiregulin	2.062	1.4E-13	2.0E-11
DUSP8	dual specificity phosphatase 8	2.060	1.4E-13	2.0E-11
HSPA1B	heat shock 70kDa protein 1B	2.041	1.4E-13	2.0E-11
Down regulated gene				
MAP4K1	mitogen-activated protein kinase kinase kinase kinase 1	-2.166	1.4E-13	2.0E-11

**(cont'd) Table 3. List of Kyoto Encyclopedia of Genes and Genomes (KEGG) pathway-enriched genes**

KIT	v-kit Hardy-Zuckerman 4 feline sarcoma viral oncogene homolog	-2.565	1.4E-13	2.0E-11
MET	MET proto-oncogene, receptor tyrosine kinase	-2.580	1.4E-13	2.0E-11
MAP3K5	mitogen-activated protein kinase kinase kinase 5	-2.734	1.4E-13	2.0E-11
MECOM	MDS1 and EVI1 complex locus	-3.228	1.4E-13	2.0E-11
MAP2K6	mitogen-activated protein kinase kinase 6	-4.599	1.4E-13	2.0E-11
2. PI3K-Akt signaling pathway				
Up regulated gene				
CASP9	caspase 9	5.007	2.1E-09	1.3E-07
NR4A1	nuclear receptor subfamily 4, group A, member 1	4.989	2.1E-09	1.3E-07
PCK1	phosphoenolpyruvate carboxykinase 1 (soluble)	4.239	2.1E-09	1.3E-07
EPHA2	EPH receptor A2	4.005	2.1E-09	1.3E-07
AREG	amphiregulin	2.480	2.1E-09	1.3E-07
GNG5	guanine nucleotide binding protein (G protein), gamma 5	2.296	2.1E-09	1.3E-07
IL6R	interleukin 6 receptor	2.185	2.1E-09	1.3E-07
SGK1	serum/glucocorticoid regulated kinase 1	2.167	2.1E-09	1.3E-07
Down regulated gene				
CSH2	chorionic somatomammotropin hormone 2	-2.066	2.1E-09	1.3E-07
CDK6	cyclin-dependent kinase 6	-2.111	2.1E-09	1.3E-07

**(cont'd) Table 3. List of Kyoto Encyclopedia of Genes and Genomes (KEGG) pathway-enriched genes**

ITGA8	integrin alpha 8	-2.506	2.1E-09	1.3E-07
KIT	v-kit Hardy-Zuckerman 4 feline sarcoma viral oncogene homolog	-2.565	2.1E-09	1.3E-07
MET	MET proto-oncogene, receptor tyrosine kinase	-2.580	2.1E-09	1.3E-07
DDIT4	DNA damage inducible transcript 4	-2.609	2.1E-09	1.3E-07
ITGA2	integrin, alpha 2 (CD49B, alpha 2 subunit of VLA-2 receptor)	-2.693	2.1E-09	1.3E-07
3. TNF signaling pathway				
Up regulated gene				
JUNB	jun B proto-oncogene	10.220	1.9E-04	1.8E-03
PTGS2	prostaglandin-endoperoxide synthase 2 (prostaglandin G/H synthase and cyclooxygenase)	6.749	1.9E-04	1.8E-03
FOS	FBJ murine osteosarcoma viral oncogene homolog	2.737	1.9E-04	1.8E-03
JUN	jun proto-oncogene	2.172	1.9E-04	1.8E-03
Down regulated gene				
MAP3K5	mitogen-activated protein kinase kinase kinase 5	-2.734	1.9E-04	1.8E-03
MAP2K6	mitogen-activated protein kinase kinase 6	-4.599	1.9E-04	1.8E-03
4. FoxO signaling pathway				
Up regulated gene				
GADD45B	growth arrest and DNA-damage-inducible, beta	14.251	4.6E-04	4.0E-03
PCK1	phosphoenolpyruvate carboxykinase 1 (soluble)	4.239	4.6E-04	4.0E-03



**(cont'd) Table 3. List of Kyoto Encyclopedia of Genes and Genomes (KEGG) pathway-enriched genes**

HOMER1	homer scaffolding protein 1	3.329	4.6E-04	4.0E-03
PLK2	polo-like kinase 2	2.373	4.6E-04	4.0E-03
SGK1	serum/glucocorticoid regulated kinase 1	2.167	4.6E-04	4.0E-03
Down regulated gene				
SOD2	superoxide dismutase 2, mitochondrial	-3.144	4.6E-04	4.0E-03
5. Wnt signaling pathway				
Up regulated gene				
FOSL1	FOS-like antigen 1	13.687	7.1E-04	5.7E-03
JUN	jun proto-oncogene	2.172	7.1E-04	5.7E-03
DKK1	dickkopf WNT signaling pathway inhibitor 1	2.040	7.1E-04	5.7E-03
Down regulated gene				
CAMK2D	calcium/calmodulin-dependent protein kinase II delta	-2.039	7.1E-04	5.7E-03
TBL1XR1	transducin (beta)-like 1 X-linked receptor 1	-2.471	7.1E-04	5.7E-03
WNT5A	wingless-type MMTV integration site family, member 5A	-2.610	7.1E-04	5.7E-03
6. Hippo signaling pathway				
Up regulated gene				
CTGF	connective tissue growth factor	4.269	9.0E-04	6.6E-03
AREG	amphiregulin	2.480	9.0E-04	6.6E-03

**(cont'd) Table 3. List of Kyoto Encyclopedia of Genes and Genomes (KEGG) pathway-enriched genes**

Down regulated gene				
DLG3	discs, large homolog 3 (Drosophila)	-2.106	9.0E-04	6.6E-03
FAT4	FAT atypical cadherin 4	-2.182	1.3E-01	2.9E-01
AMOT	angiomin	-2.362	9.0E-04	6.6E-03
YAP1	Yes-associated protein 1	-2.370	9.0E-04	6.6E-03
WNT5A	wingless-type MMTV integration site family, member 5A	-2.610	9.0E-04	6.6E-03
7. cGMP-PKG signaling pathway				
Up regulated gene				
ATP1B3	ATPase, Na <sup>+</sup> /K <sup>+</sup> transporting, beta 3 polypeptide	2.020	7.7E-03	3.7E-02
Down regulated gene				
GUCY1B3	guanylate cyclase 1, soluble, beta 3	-2.052	7.7E-03	3.7E-02
PDE5A	phosphodiesterase 5A, cGMP-specific	-2.149	7.7E-03	3.7E-02
ATP2B4	ATPase, Ca <sup>++</sup> transporting, plasma membrane 4	-2.186	7.7E-03	3.7E-02
GUCY1A3	guanylate cyclase 1, soluble, alpha 3	-2.950	7.7E-03	3.7E-02
8. ErbB signaling pathwa				
Up regulated gene				
AREG	amphiregulin	2.480	8.0E-03	3.8E-02
HBEGF	heparin-binding EGF-like growth factor	2.376	8.0E-03	3.8E-02

**(cont'd) Table 3. List of Kyoto Encyclopedia of Genes and Genomes (KEGG) pathway-enriched genes**

JUN	jun proto-oncogene	2.172	8.0E-03	3.8E-02
Down regulated gene				
CAMK2D	calcium/calmodulin-dependent protein kinase II delta	-2.039	8.0E-03	3.8E-02
9. Ras signaling pathway				
Up regulated gene				
EPHA2	EPH receptor A2	4.005	2.4E-02	8.7E-02
RGL1	ral guanine nucleotide dissociation stimulator-like 1	2.682	2.4E-02	8.7E-02
GNG5	guanine nucleotide binding protein (G protein), gamma 5	2.296	2.4E-02	8.7E-02
Down regulated gene				
KIT	v-kit Hardy-Zuckerman 4 feline sarcoma viral oncogene homolog	-2.565	2.4E-02	8.7E-02
MET	MET proto-oncogene, receptor tyrosine kinase	-2.580	2.4E-02	8.7E-02
10. cAMP signaling pathway				
Up regulated gene				
FOS	FBJ murine osteosarcoma viral oncogene homolog	2.737	1.5E-02	5.9E-02
JUN	jun proto-oncogene	2.172	1.5E-02	5.9E-02
ATP1B3	ATPase, Na <sup>+</sup> /K <sup>+</sup> transporting, beta 3 polypeptide	2.020	1.5E-02	5.9E-02
Down regulated gene				
CAMK2D	calcium/calmodulin-dependent protein kinase II delta	-2.039	1.5E-02	5.9E-02

**(cont'd) Table 3. List of Kyoto Encyclopedia of Genes and Genomes (KEGG) pathway-enriched genes**

ATP2B4	ATPase, Ca <sup>++</sup> transporting, plasma membrane 4	-2.186	1.5E-02	5.9E-02
11. mTOR signaling pathway				
Up regulated gene				
SGK1	serum/glucocorticoid regulated kinase 1	2.167	3.5E-02	1.1E-01
SLC3A2	solute carrier family 3 (amino acid transporter heavy chain), member 2	2.021	3.5E-02	1.1E-01
Down regulated gene				
DDIT4	DNA damage inducible transcript 4	-2.609	3.5E-02	1.1E-01
WNT5A	wingless-type MMTV integration site family, member 5A	-2.610	3.5E-02	1.1E-01

**Table 4. Body weight and fasting blood glucose in lean and Diet-Induced Obese (DIO) mice.**  
**C57BL/6J (Male)**

Lean			DIO		
Number	Body weight (g)	Fasting glucose (mM)	Number	Body weight (g)	Fasting glucose (mM)
1	35	94	1	63	133
2	36	73	2	61	144
3	34	82	3	66	142
4	35	82	4	68	147
5	33	84	5	66	157
6	32	83	6	68	145

## 국문 초록

제 2 형 당뇨병은 고혈당을 특징으로 하는 일련의 대사성 질환을 통칭한다. 오늘날까지, 고혈당을 조절하는 약물들의 메커니즘은 알려져 있지만, 인슐린 저항성과 합병증을 조절하는 메커니즘에 대해서는 거의 알려져 있지 않다.

프로키네티신 수용체 1 의 활성화는 백색 지방의 양을 줄이고, 조직에 혈관을 통한 인슐린 전달 작용을 강화시킨다. 또 심근 경색 생존율을 증가시킴으로써 비만 및 당뇨병 합병증인 심혈관계 질환을 개선시킨다. 그러나 프로키네티신 수용체 1 이 골격근에서 미치는 영향은 아직 연구가 되지 않았다. 본 연구에서는 근모 세포와 근 위성 세포를 이용하여 골격근에서 인슐린 저항성에 대한 프로키네티신 수용체 1 의 역할을 조사했다.

근모 세포와 근위성세포의 분화과정에서 프로키네티신 수용체 1 의 발현 정도를 조사하였고, 그 결과 근세포가 근관 세포로 분화될수록 단백질 수준의 프로키네티신 수용체 1 의 수준이 증가함을 확인했다. 프로키네티신 수용체 1 과 발현 신장세포주를 통해 칼슘 이동 실험을 해본 결과, 프로키네티신 수용체 1 의 천연 단백질인 프로키네티신 2 는 농도 의존적으로 세포 내 칼슘 이동을

유도하여 프로키네티신 수용체 1 이 Gq 단백질과 결합되는 것을 확인했다. 프로키네티신 수용체 1 과발현 신장세포주에 프로키네티신 2 처리에 하여 발현된 유전자차이를 알아보기 위해 microarray datasets 의 분석을 진행했다. 프로키네티신 수용체 1 활성화에 의해 총 578 개의 발현된 유전자차이를 확인했으며, 309 개의 하향 조절된 유전자와 296 개의 유전자를 확인했다. 발현된 유전자 차이가 어떠한 생물학적 의미를 동정해본 결과, 프로키네티신 수용체 1 이 PI3K/Akt 신호전달경로와 MAPK/Erk 신호전달경로를 활성화시킬 것이라는 가설을 세웠다.

세포실험에서 프로키네티신 수용체 1 은 인슐린의 존재 여부에 관계없이 근모세포와 근위성세포에서 유래된 근관에서 PI3K/Akt 신호 전달 경로를 유의하게 활성화시켰다. 또한, 프로키네티신 수용체 1 의 활성화는 근모세포와 근위성세포에서 유래된 근관에서 포도당 수용체 4 의 전이를 증가시켰고, 그에 따라 포도당 흡수를 증가시켰다. 포화지방산에 의해 인슐린 저항성이 유도된 근관에서 프로키네티신 수용체 1 의 활성화는 PI3K/Akt 인산화를 회복시켰고, 포도당수용체 4 의 세포막으로의 전이를 증가시켰으며, 포도당흡수를 정상수준까지 증가시켰다.

결과적으로 포화지방산에 의해 유도된 인슐린 저항성이 유도된 근관에서 프로키네티신 수용체 1 에 의해 인슐린 민감도가

향상되었다. 동물실험에서, 프로키네티신 수용체 1의 단백질 골격근 조직과 백색지방 조직에서 정상 마우스에 대비하여 비만 마우스의 단백질 수준이 감소하는 것을 확인했다.

이러한 결과를 종합해 볼 때, 프로키네티신 수용체 1은 골격근에서 인슐린 저항성을 개선시켰고, 프로키네티신 수용체 1이 제 2형 당뇨병에서 인슐린 저항성 치료적 표적이 될 수 있음을 시사한다.



## References

1. Mancia, G., *Preventing new-onset diabetes in thiazide-treated patients*. Lancet Diabetes Endocrinol, 2016. **4**(2): p. 90-2.
2. Alberti, K.G. and P.Z. Zimmet, *Definition, diagnosis and classification of diabetes mellitus and its complications. Part 1: diagnosis and classification of diabetes mellitus provisional report of a WHO consultation*. Diabet Med, 1998. **15**(7): p. 539-53.
3. Laakso, M., *Cardiovascular disease in type 2 diabetes from population to man to mechanisms: the Kelly West Award Lecture 2008*. Diabetes Care, 2010. **33**(2): p. 442-9.
4. Chaudhury, A., et al., *Clinical Review of Antidiabetic Drugs: Implications for Type 2 Diabetes Mellitus Management*. Front Endocrinol (Lausanne), 2017. **8**: p. 6.
5. <https://www.prnewswire.com/news-releases/the-global-proposal-management-software-market-size-is-projected-to-grow-from-usd-1-5-billion-in-2019-to-usd-3-1-billion-by-2024--at-a-compound-annual-growth-rate-cagr-of-14-9-300958451.html>.
6. Rabizadeh, S., M. Nakhjavani, and A. Esteghamati, *Cardiovascular and Renal Benefits of SGLT2 Inhibitors: A Narrative Review*. Int J Endocrinol Metab, 2019. **17**(2): p. e84353.
7. Kahn, B.B. and J.S. Flier, *Obesity and insulin resistance*. J Clin Invest, 2000. **106**(4): p. 473-81.
8. Leney, S.E. and J.M. Tavaré, *The molecular basis of insulin-stimulated glucose uptake: signalling, trafficking and potential drug targets*. J Endocrinol, 2009. **203**(1): p. 1-18.
9. Niswender, K.D., et al., *Insulin activation of phosphatidylinositol 3-kinase in the hypothalamic arcuate nucleus: a key mediator of insulin-induced anorexia*. Diabetes, 2003. **52**(2): p. 227-31.
10. Miinea, C.P., et al., *AS160, the Akt substrate regulating GLUT4 translocation, has a functional Rab GTPase-activating protein domain*. Biochem J, 2005. **391**(Pt 1): p. 87-93.

11. DeFronzo, R.A., *Pathogenesis of type 2 diabetes mellitus*. Med Clin North Am, 2004. **88**(4): p. 787-835, ix.
12. DeFronzo, R.A., *Banting Lecture. From the triumvirate to the ominous octet: a new paradigm for the treatment of type 2 diabetes mellitus*. Diabetes, 2009. **58**(4): p. 773-95.
13. Reaven, G.M., et al., *Measurement of plasma glucose, free fatty acid, lactate, and insulin for 24 h in patients with NIDDM*. Diabetes, 1988. **37**(8): p. 1020-4.
14. Qvigstad, E., et al., *Acute lowering of circulating fatty acids improves insulin secretion in a subset of type 2 diabetes subjects*. Am J Physiol Endocrinol Metab, 2003. **284**(1): p. E129-37.
15. Ahren, B., *Reducing plasma free fatty acids by acipimox improves glucose tolerance in high-fat fed mice*. Acta Physiol Scand, 2001. **171**(2): p. 161-7.
16. Mauro, A., *Satellite cell of skeletal muscle fibers*. J Biophys Biochem Cytol, 1961. **9**: p. 493-5.
17. Yin, H., F. Price, and M.A. Rudnicki, *Satellite cells and the muscle stem cell niche*. Physiol Rev, 2013. **93**(1): p. 23-67.
18. Collins, C.A., et al., *Stem cell function, self-renewal, and behavioral heterogeneity of cells from the adult muscle satellite cell niche*. Cell, 2005. **122**(2): p. 289-301.
19. Seale, P., et al., *Pax7 is required for the specification of myogenic satellite cells*. Cell, 2000. **102**(6): p. 777-86.
20. Cornelison, D.D. and B.J. Wold, *Single-cell analysis of regulatory gene expression in quiescent and activated mouse skeletal muscle satellite cells*. Dev Biol, 1997. **191**(2): p. 270-83.
21. Relaix, F. and P.S. Zammit, *Satellite cells are essential for skeletal muscle regeneration: the cell on the edge returns centre stage*. Development, 2012. **139**(16): p. 2845-56.
22. Musaro, A. and S. Carosio, *Isolation and Culture of Satellite Cells from Mouse Skeletal Muscle*. Methods Mol Biol, 2017. **1553**: p. 155-167.
23. Day, K., et al., *Nestin-GFP reporter expression defines the quiescent state of skeletal muscle satellite cells*. Dev Biol, 2007. **304**(1): p. 246-59.

24. Blau, H.M., et al., *Plasticity of the differentiated state*. Science, 1985. **230**(4727): p. 758-66.
25. Yaffe, D. and O. Saxel, *Serial passaging and differentiation of myogenic cells isolated from dystrophic mouse muscle*. Nature, 1977. **270**(5639): p. 725-7.
26. Chaturvedi, V., et al., *Interactions between Skeletal Muscle Myoblasts and their Extracellular Matrix Revealed by a Serum Free Culture System*. PLoS One, 2015. **10**(6): p. e0127675.
27. Grabowska, I., et al., *Comparison of satellite cell-derived myoblasts and C2C12 differentiation in two- and three-dimensional cultures: changes in adhesion protein expression*. Cell Biol Int, 2011. **35**(2): p. 125-33.
28. Lorsch, J.R., F.S. Collins, and J. Lippincott-Schwartz, *Cell Biology. Fixing problems with cell lines*. Science, 2014. **346**(6216): p. 1452-3.
29. Chaly, A.L., et al., *The Melanocortin Receptor Accessory Protein 2 promotes food intake through inhibition of the Prokineticin Receptor-1*. Elife, 2016. **5**.
30. Dormishian, M., et al., *Prokineticin receptor-1 is a new regulator of endothelial insulin uptake and capillary formation to control insulin sensitivity and cardiovascular and kidney functions*. J Am Heart Assoc, 2013. **2**(5): p. e000411.
31. Beale, K., et al., *Peripheral administration of prokineticin 2 potently reduces food intake and body weight in mice via the brainstem*. Br J Pharmacol, 2013. **168**(2): p. 403-10.
32. Lin, D.C., et al., *Identification and molecular characterization of two closely related G protein-coupled receptors activated by prokineticins/endocrine gland vascular endothelial growth factor*. J Biol Chem, 2002. **277**(22): p. 19276-80.
33. Kaser, A., et al., *The AVIT protein family. Secreted cysteine-rich vertebrate proteins with diverse functions*. EMBO Rep, 2003. **4**(5): p. 469-73.
34. Szatkowski, C., et al., *Prokineticin receptor 1 as a novel suppressor of preadipocyte proliferation and differentiation to control obesity*. PLoS One, 2013. **8**(12): p. e81175.
35. Urayama, K., et al., *The prokineticin receptor-1 (GPR73) promotes cardiomyocyte survival and angiogenesis*. Faseb j, 2007. **21**(11): p. 2980-93.

36. Boulberdaa, M., et al., *Genetic inactivation of prokineticin receptor-1 leads to heart and kidney disorders*. Arterioscler Thromb Vasc Biol, 2011. **31**(4): p. 842-50.
37. Longo, M., et al., *Adipose Tissue Dysfunction as Determinant of Obesity-Associated Metabolic Complications*. Int J Mol Sci, 2019. **20**(9).
38. Cao, Y., *Angiogenesis and vascular functions in modulation of obesity, adipose metabolism, and insulin sensitivity*. Cell Metab, 2013. **18**(4): p. 478-89.
39. Genders, A.J., et al., *Endothelial cells actively concentrate insulin during its transendothelial transport*. Microcirculation, 2013. **20**(5): p. 434-9.
40. Cao, Y., *Adipose tissue angiogenesis as a therapeutic target for obesity and metabolic diseases*. Nat Rev Drug Discov, 2010. **9**(2): p. 107-15.
41. LeCouter, J. and N. Ferrara, *EG-VEGF and the concept of tissue-specific angiogenic growth factors*. Semin Cell Dev Biol, 2002. **13**(1): p. 3-8.
42. Urayama, K., et al., *Prokineticin receptor-1 induces neovascularization and epicardial-derived progenitor cell differentiation*. Arterioscler Thromb Vasc Biol, 2008. **28**(5): p. 841-9.
43. Pasut, A., A.E. Jones, and M.A. Rudnicki, *Isolation and culture of individual myofibers and their satellite cells from adult skeletal muscle*. J Vis Exp, 2013(73): p. e50074.
44. Pajtler, K., et al., *Production of chick embryo extract for the cultivation of murine neural crest stem cells*. J Vis Exp, 2010(45).
45. Wang, X., et al., *Palmitate induced insulin resistance by PKC $\theta$ -dependent activation of mTOR/S6K pathway in C2C12 myotubes*. Exp Clin Endocrinol Diabetes, 2010. **118**(9): p. 657-61.
46. van Rijn, R.M., et al., *Novel screening assay for the selective detection of G-protein-coupled receptor heteromer signaling*. J Pharmacol Exp Ther, 2013. **344**(1): p. 179-88.
47. Zierath, J.R., et al., *Insulin action on glucose transport and plasma membrane GLUT4 content in skeletal muscle from patients with NIDDM*. Diabetologia, 1996. **39**(10): p. 1180-9.

48. Brown, D.M., T. Parr, and J.M. Brameld, *Myosin heavy chain mRNA isoforms are expressed in two distinct cohorts during C2C12 myogenesis*. J Muscle Res Cell Motil, 2012. **32**(6): p. 383-90.
49. Neves, S.R., P.T. Ram, and R. Iyengar, *G protein pathways*. Science, 2002. **296**(5573): p. 1636-9.
50. Berridge, M.J., *Inositol trisphosphate and calcium signalling*. Nature, 1993. **361**(6410): p. 315-25.
51. Leto, D. and A.R. Saltiel, *Regulation of glucose transport by insulin: traffic control of GLUT4*. Nat Rev Mol Cell Biol, 2012. **13**(6): p. 383-96.
52. Navratil, J., *[Use of the operating microscopy in septorhinoplasty]*. Cesk Otolaryngol, 1987. **36**(2): p. 75-7.
53. Kim, S., G.W. Go, and J.Y. Imm, *Promotion of Glucose Uptake in C2C12 Myotubes by Cereal Flavone Tricin and Its Underlying Molecular Mechanism*. J Agric Food Chem, 2017. **65**(19): p. 3819-3826.
54. Arora, H., et al., *Prokineticin receptor-1 signaling promotes Epicardial to Mesenchymal Transition during heart development*. Sci Rep, 2016. **6**: p. 25541.
55. Gasser, A., et al., *Discovery and cardioprotective effects of the first non-Peptide agonists of the G protein-coupled prokineticin receptor-1*. PLoS One, 2015. **10**(4): p. e0121027.
56. Yang, M., et al., *Saturated fatty acid palmitate-induced insulin resistance is accompanied with myotube loss and the impaired expression of health benefit myokine genes in C2C12 myotubes*. Lipids Health Dis, 2013. **12**: p. 104.
57. Park, C.E., et al., *Resveratrol stimulates glucose transport in C2C12 myotubes by activating AMP-activated protein kinase*. Exp Mol Med, 2007. **39**(2): p. 222-9.
58. Meng, S., et al., *TBX20 Regulates Angiogenesis Through the Prokineticin 2-Prokineticin Receptor 1 Pathway*. Circulation, 2018. **138**(9): p. 913-928.
59. Rockman, H.A. and R.J. Lefkowitz, *Introduction to the series on novel aspects of cardiovascular G-protein-coupled receptor signaling*. Circ Res, 2011. **109**(2): p. 202-4.

## 감사의 글

삶에 변화를 주고자 시작한 3년 동안의 여정을 마치고 석사 졸업이라는 작은 목적지에 다다르려고 합니다. 긴 여정에 도움을 주신 모든 분들께 감사의 마음을 전하려 합니다. 그 동안 부족한 저에게 많은 도움을 주신 주위 분들의 덕분에 지금의 자리에 있을 수 있게 되었습니다.

먼저 바쁘신 가운데에도 제 학위논문의 심사위원을 맡아 주시고 좋은 조언을 해 주신 두 분께 감사드립니다.

제 연구들의 대부분을 공동으로 지도해 주시고 그 간 날카로운 코멘트들로 제게 큰 도움을 주셨던 박태섭 교수님, 항상 저희 디자인 동물 이식 연구소를 위해 고생해 주시고 많은 좋은 말씀 해주신 염수청 교수님께 큰 감사를 드립니다.

그리고 아직도 많이 부족한 저에게 배움의 기회를 주셨던 박중훈 교수님께 감사인사 올립니다. 항상 쫓지 말라며, 자신감 있게 실험하라고 지도해 주셔서, 이만큼 성장할 수 있었습니다. 학문적인 방향 뿐 만이 아닌 제가 선택한 분야에 자부심을 느낄 수 있게 해주셔서, 매순간 지치지 않고 달려올 수 있었습니다. 그동안 교수님의 좋은 말씀과 사랑이 제게는 소중한 추억이며 잊을 수 없는 시간이 될 것 같습니다. 앞으로도 박중훈 교수님 이름에 드높힐 수 있는 제자 목종수가 되겠습니다.

다시 한번 깊이 감사드립니다.

제가 처음으로 이 분야에 관심을 갖게 해주신 분이자 대학원 진학에 있어서 각별히 생각하고 조언해 주셨던 학부 지도 교수님 김동환 교수님께 감사드립니다. 언제든지 반갑게 맞아 주시며 소중한 조언과 인생 상담을 해주신

교수님께 감사 드립니다. 모든 면에서 무한한 도움을 주셨습니다. 정말 감사드립니다.

가족 같은 분위기로 저의 엔돌핀이 되어 주었던 실험실 구성원 분들 장춘건, 김은서, 성연우 학생, 한영인 선생님에게도 감사를 드립니다.

마지막으로 항상 저를 믿어 주시고 무엇에 도전하든 용기를 주시는 저의 소중한 부모님께 감사드립니다. 제멋대로인 아들인데 항상 이해해 주시고 믿어주셔서 제가 여기까지 할 수 있었고, 한 발짝 더 나아가겠다는 결심도 할 수 있었습니다. 열심히, 그리고 잘 하여서 부모님께서 해주신 은혜에 보답할 수 있는 자랑스러운 아들이 되도록 하겠습니다.

이외에도 여기에 미처 적지 못한 많은 분들께 감사드립니다. 여러분이 있어 제가 있었고, 저도 여러분께 힘이 될 수 있는 존재가 될 수 있도록 하겠습니다. 감사하고 사랑합니다.

목종수 올림.